Special Issue IJEAR Vol. 11 No 2 : **February 2025**

Proceedings of International Conference on Electronics and Advances in Science & Technology, (IConEAST-24)

Nov. 8-9, 2024

Towards mitigating natural hazards for a better humanosphere

Venue : Gauhati University, India

Space borne Aerosol and Carbon dioxide Detection Lidar (ACDL) : Status and Results

Weibiao Chen*, JiqiaoLiu, Xia Hou, Xiaopeng Zhu, Yuan Wan, Xihuhua Ma
Shanghai Institute of Optics and Fine Mechanics, Chinese Academy of Sciences,
No. 390 Qinghe Rd., Jiading, Shanghai 201800, China
e-mail: wbchen@siom.ac.cn

Article History : *1st received: 14.12.2024 Final : 25.12.2024*

Abstract:

Spaceborne Aerosol and Carbon dioxide Detection Lidar (ACDL) was developed and launched on April 16th, 2022. ACDL integrated two kinds of lidar systems with a 1572 nm integrated path laser differential absorption (IPDA) to measure the global CO_2 column concentrations (XCO_2), and a 532 nm high spectral resolution lidar (HSRL) method to measure aerosols and clouds. The global XCO_2 and aerosol profiles from 82° N to 82° S over land and sea in the daytime and nighttime are presented.

***Keywords** : Aerosol and Carbon Dioxide Detection Lidar, AEMS, Total Carbon Column Observing Network (TCCON) sites, Column Concentration*

This is a part of keynote speech delivered by **Prof. Weibiao Chen** at the International Conference on Electronics and Advances in Science & Technology (IConEAST-24) held during Nov. 8 and 9, 2024, at Gauhati University, Guwahati, India.

1. Introduction

Space-borne lidar for active monitoring of greenhouse gases could operate all day, have a high probability of penetrating clouds, and are hardly affected by aerosols. High-precision monitoring of global greenhouse gas CO_2 and aerosol concentration are important for environmental monitoring and climate change research.

ACDL is the main payload of the AEMS satellite, which is operating in a sun-synchronous orbit at 705 km altitude. The orbit inclination of 98.2° provides global coverage between 82°N and 82°S.The main goal is to obtain global atmospheric CO_2 column concentration distribution, then provide quantitative scientific data for the accurate assessment of CO_2 sources and sinks [Liu et al ., 2021]. The second goal is to measure the vertical profiles of global atmospheric aerosols and clouds with high accuracy, and to study their impact and role in monitoring air quality and global climate change. ACDL has achieved innovative breakthroughs: the first space-borne global CO_2 concentration measurement lidar and the first space-borne HSRL based Iodine filter for atmospheric aerosols and cloud profiles measurements. The main parameters and on-orbit performance will be shown. High accuracy XCO_2 and aerosol profiles measurements are presented.

2. ACDL description

ACDL uses HSRL detection technology to measure the optical parameters profiles of the atmosphere aerosols and clouds [Dong et al., 2018; Liu et al., 2019], and uses IPDA technology to measure CO_2 column concentration [Xia et al., 2022]. The two different lidar principles are integrated into the ACDL lidar to measure CO_2 and aerosols and clouds simultaneously.

The lidar emits triple-wavelength (532 nm/1064 nm/1572 nm) frequency stabilized double-pulses from the same power laser, and the time interval of double pulses is 200 μs with repetition rate of 20 Hz. The laser transmitter consists of frequency stabilization seeders, three wavelength pulsed lasers, a pointing control mirror and a beam expander. The CW seeder at 1572 nm is locked to the CO_2 cell with stability of 0.3 MHz, and the seeder laser at 1064 nm is frequency-doubled to obtain 532 nm and locked to the iodine cell line with stability of 0.5 MHz. The Transmitter energies are 150 mJ@532 nm, 130 mJ @1064 nm, and 75 mJ @1572 nm, respectively.

The lidar system is coaxial,and the transmitter axis pointing could be adjusted to match the field of view (FOV). The diameter of the receiver telescope is 1 m with FOV of 0.15 mrad. The lidar receiver consists of a 1572 nm detector, a 1064 nm detector, and three 532 nm detectors. Three 532 nm channels consist of an HSRL channel with iodine cell, and parallel, perpendicular polarization channels. Figure 1 is the setup of ACDL.

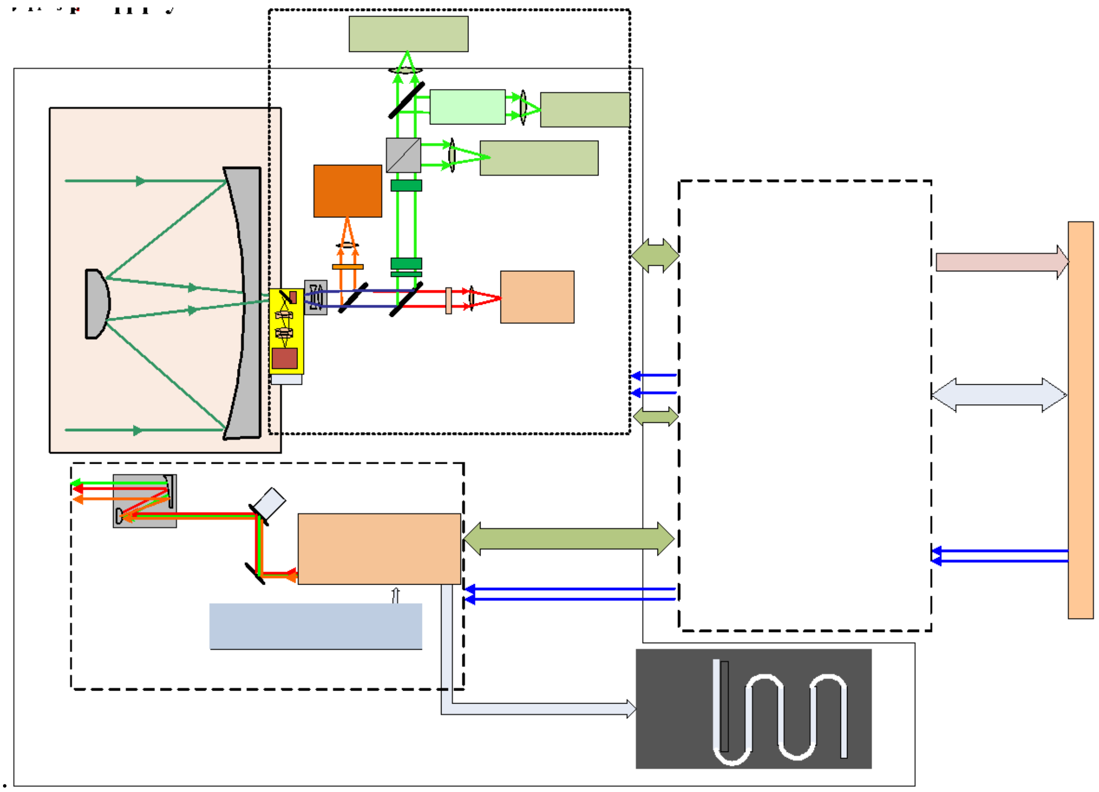

Figure 1: Schematic diagram of ACDL lidar

3. On-orbit Measurement

ACDL was launched in April, 2022. It has been implemented for more than 2 years. Laser transmitter, detection performance keeps stability. The Allan deviation of laser stability is less than 0.03 MHz. The on-orbit performance of ACDL's laser is shown as in Figure.2. The laser pointing stability is quite important for lidar observation. The optical axis monitoring in lidar is set up. The axis changing of the transceiver is less than 5 μrad between before and after launching. An in-situ campaign to measure laser point was also conducted in the grassland of Inner Mongolia, we found the bias error is less than 2.5 m compared to the estimated pointing. The results are shown in Figure-3.

(a) Laser energy

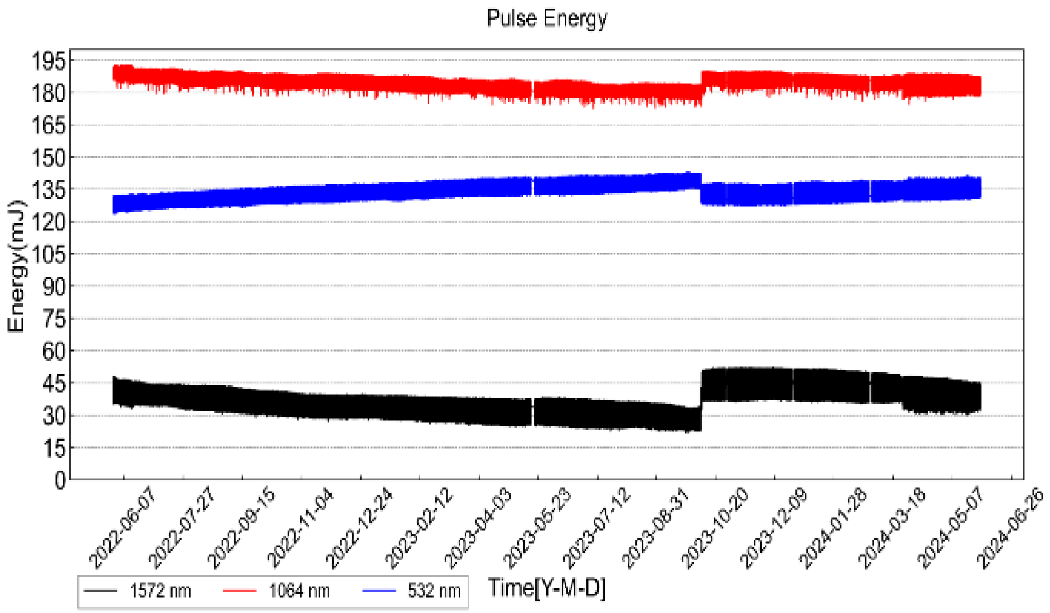

(b) Laser frequency stability

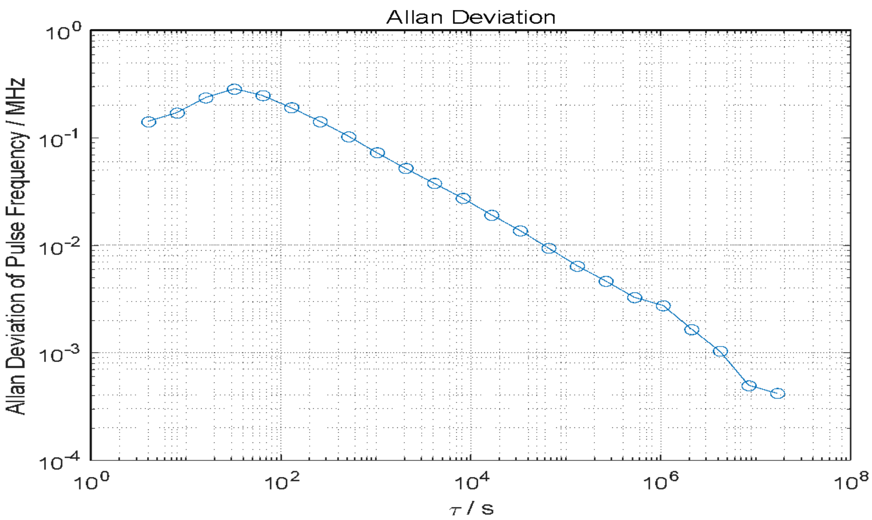

Figure 2: On-orbit performance of ACDL

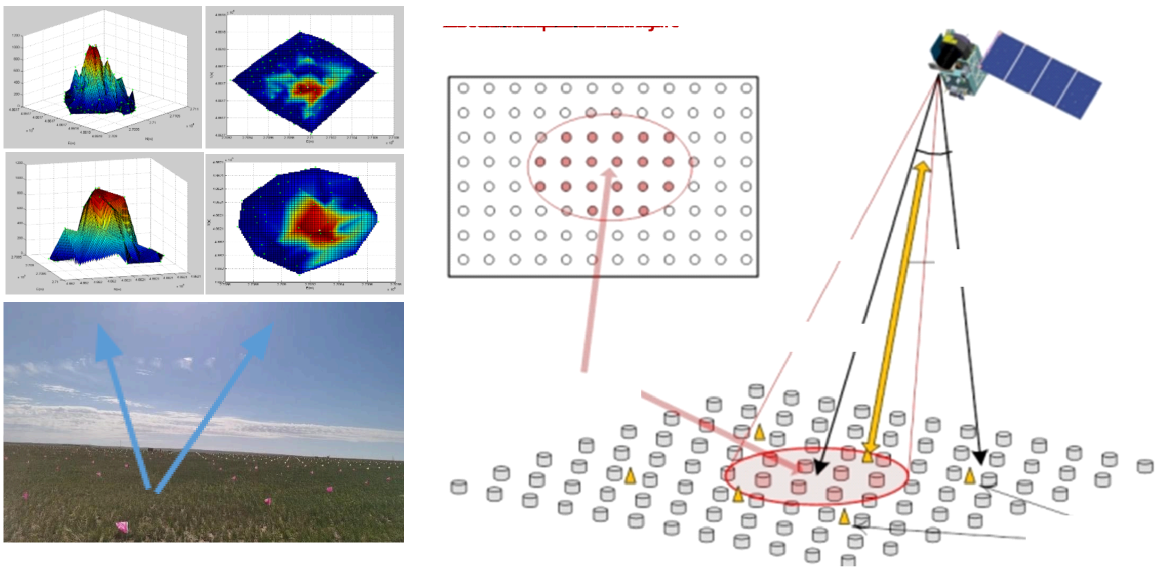

Calibration	B (°)	L (°)	N (m)	E (m)	H (m)	Geometric plane error)
Calculated coordinates	43.8789539	114.1477699	4862383.611	270856.746	1029.298	
Measured coordinates	43.87896121	114.1477964	4862384.350	270858.906	1028.581	
Error			0.735	2.160	-0.717	2.282

Figure 3 : Lidar pointing campaign in Inner Mongolia

4. Data Product of CO_2, Aerosol and Cloud

After calibration, verification was done of the data product of column concentration of CO_2, optical thickness of aerosol and cloud, the topography of earth, and top height of cloud. The typical data products of Level 2A at 532 nm are shown in Figure 4 (a,b,c), including the attenuated backscatter coefficient profiles of aerosols and clouds obtained from parallel channel, polarization channel and HSRL channel. The XCO_2 distribution in June 2022 measured by the ACDL in days and nights with a 1°×1°grid is also shown in Figure 1(d). The space-borne lidar has obtained CO_2 column concentration data with high coverage, because the laser could penetrate thin clouds and could use backscattered signals from thick clouds. The XCO_2 measured accuracy is validated to be less than 1 ppm when compared to XCO_2 data from TCCON sites. As the first space-borne CO_2 detection lidar and first aerosol measurement HSRL based Iodine filter, it has the ability to obtain XCO_2 in bipolar zone and in nighttime, which is useful for global climate study.

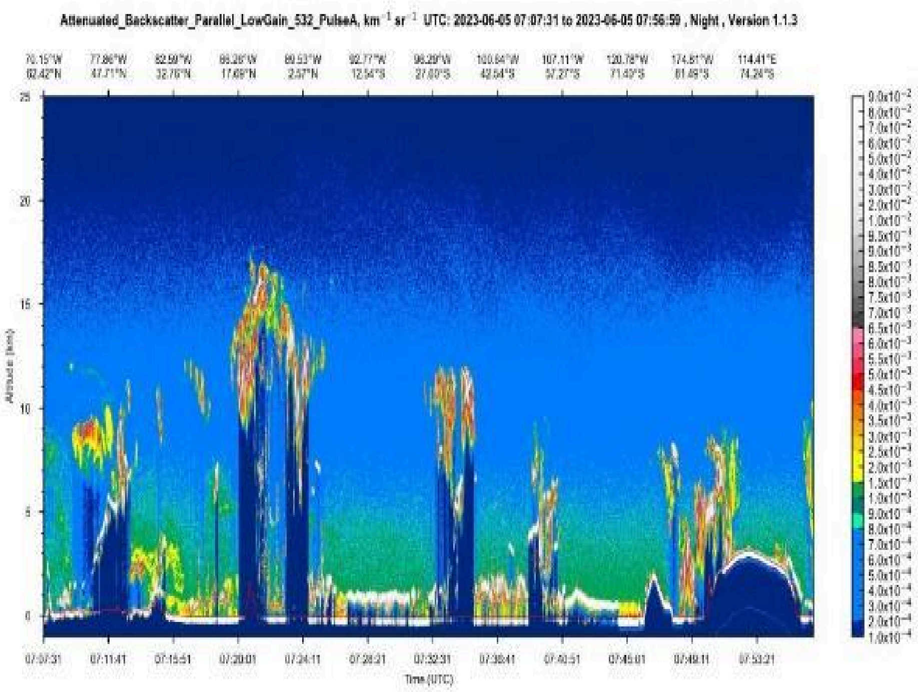

(a).

Special Issue IJEAR Vol. 11 No 2 : **February 2025**

Proceedings of International Conference on Electronics and Advances in Science & Technology, (IConEAST-24)

Nov. 8-9, 2024

Towards mitigating natural hazards for a better humanosphere

Venue : Gauhati University, India

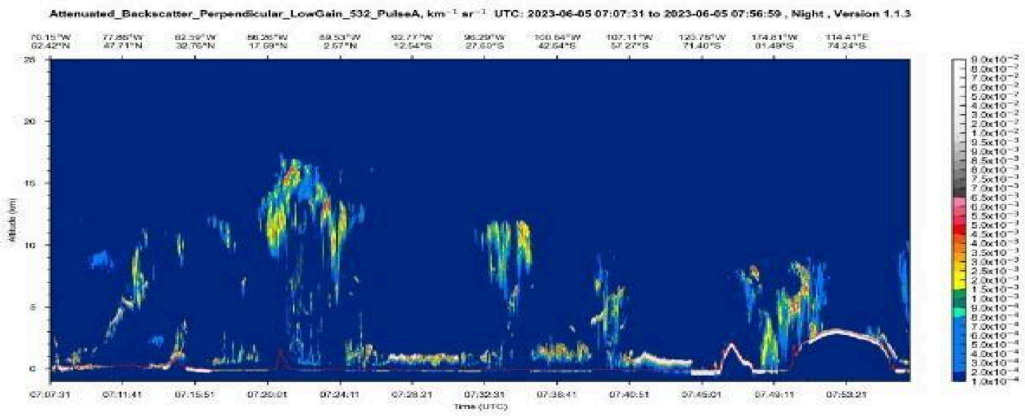

(b)

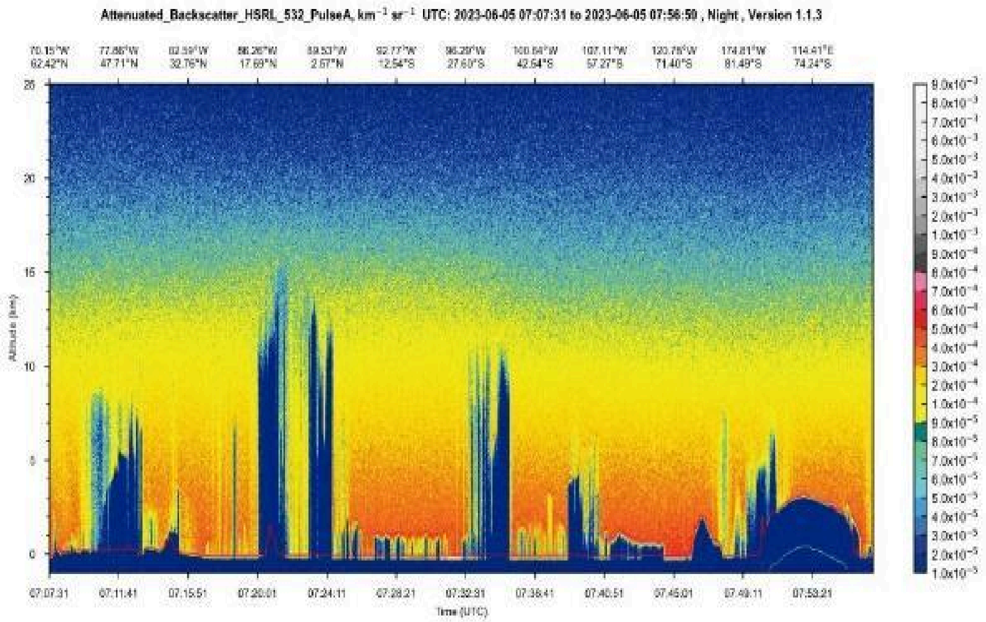

(c)

.

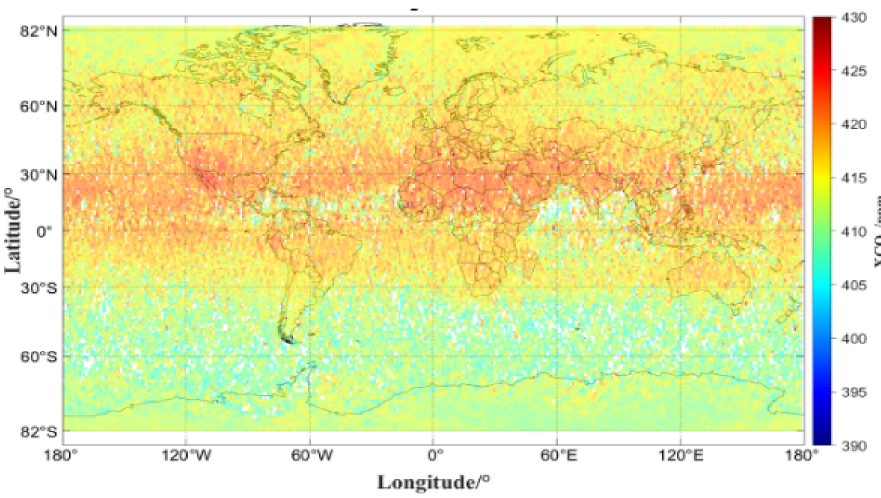

(d)

Figure 4: Attenuated backscatter coefficient of aerosol at 532 nm from parallel (a), polarization (b) and HSRL channel (c). And one month average of XCO2 with 1°×1°grid (d)

References

Dong J, Liu J, Bi D et al,(2018),Optimal iodine absorption line applied for space borne high spectral resolution lidar," *Appl. Opt*, 57,5413-5419

Liu D, Zheng Z, Chen W et al, (2019) "Performance estimation of space-borne high-spectral-resolution lidar for cloud and aerosol optical properties at 532 nm," *Opt. Express*, 27,A481-A494,

Liu Y, Wang J, Che K et al, (2021),"Satellite remote sensing of greenhouse gases: Progress and trends," *National Remote Sensing Bulletin*, 25(1),53-64

Xia T, Liu J, Zhu Z et al,(2022) "Calibration experiments based on a CO2 absorption cell for the 1.57-μm spaceborne IPDA LIDAR," *Opt. Express*, 30, 35146-35162.

.

About the author and keynote speaker

e-mail: wbchen@siom.ac.cn

Prof .Weibiao CHEN, PH.D, Professor. Director of Shanghai Institute of Optics and Fine Mechanics, Chinese Academy of Sciences. One of the executive directors of the Chinese Society of Optical Engineering. He has been involved in developing techniques of space laser, laser remote sensing for atmospheric and oceanographic, and space laser communication, et.al. As PI, he has presided over the development of the first space laser, first space borne atmospheric lidar, and first space coherent laser communication system in China. He has published more than 170 papers, 2 books, and authorized more than 80 national invention patents.

Special Issue IJEAR Vol. 11 No 2 : **February 2025**

Proceedings of International Conference on Electronics and Advances in Science & Technology, (IConEAST-24)

Nov. 8-9, 2024

Towards mitigating natural hazards for a better humanosphere

Venue : Gauhati University, India

Nanosatellites and International Collaboration on Earthquake Precursor Studies

Oyama,K.-I.[1, 2]

1. International Center for space and Planetary Environmental Sciences, Kyushu University, Fukuoka, Japan
2. Co., Ltd. Asia Space Environment Research Consortium, Kanagawa, Japan

Article History : *1st received: 12.12.2024 Final : 12.01.2025*

Abstract:

Both ground based and satellite observations which we studied so far for the large earthquakes (M> 6.5), show the existence of ionosphere modification before they occurred [Oyama and Devi,2020]. The special features in the ionosphere, such as the increase/ decrease of NmF2 (maximum density of F layer), 2 days oscillation of the NmF2 variation, which repeats 3-4 times, and the continuous decrease /decrease NmF2 before and after the earthquakes, are important aspects of study. The precursor signals also appear in the height profile of neutral temperature [Sun et al., 2011], and vertical ground motion observed with the slant gauges which suggests that the ground motion excites the atmospheric waves, and the waves modifies the E region Dynamo electric field [Oyama et al., 2024]. Although we now have firm evidence of the ionosphere disturbance before earthquakes, we still need the further evidence to predict the large earthquakes. The prediction of large earthquakes might become possible soon if we work together by bringing the data of different geophysical parameter such as NmF2, daily variation of the magnetic field caused by Sq current, electric field calculated by Doppler frequency data observed by HF radars, VLF emission from the epicenter region, vertical electric field, radon emission from the ground, and so on. It is essential to distribute these sensors in a wide area. In addition to these data, space weather data such as F10.7 solar radio flux,3-hourKp index which shows the geomagnetic variation

at rather high latitudes, and Dst, caused by ring current which flows over the geomagnetic equator are essential to discriminate the effect caused by earthquake from that caused by the natural geomagnetic disturbance.Sometimes we might need the information on meteorite shower. However, as the large earthquake about which we need to study, is very scarce in one country (though with large devastating destructive power),we surely need satellite constellation which makes it possible to study further deeper by using worldwide earthquakes [Jason et al., 2002; Korepanov et al., 2008; Oyama et al., 2010; Bankov et al, 2017; Picozza et al., 2021]. The satellite mission can contribute to the countries where ground instruments are not distributed enough to predict earthquakes**.** One satellite is not enough because we have only 22.5° resolution in longitude for the satellite altitudes of 500-600 km. The separation is not enough to confirm the phenomena observed in the previous orbit, because the location is 22.5° away from the previous orbit and the local time is also different. The satellite mission can contribute to the countries where ground instruments are not distributed enough to predict earthquakes. The manuscript describes our findings which were obtained using satellites, Hinotori, DE-2, and DMSPF1, and proposes a satellite constellation which consists of CubeSat and small satellite(s).

Keywords: *Earthquake,Precursor,Lithosphere/Atmosphere/Ionosphere,Satellite constellation*

Keynote lecture at International Conference on Electronics and Advances in Science and Technology, ICon EAST-24 (8-9, Nov. 2024), Guwahati ,India.

1. Observations

Satellite Observations

1.a. Electron temperature measurement

The Japanese sun observation satellite 'Hinotori' was put into equatorial orbit (the inclination; 30°) at the height of 600 km in February , 1981 , http://isas.ac.jp/enterp/mission/himotori.shtml). Although the satellite was dedicated to study solar physics, two unique plasma probes that were developed in Japan were accommodated. The two probes are a resonance rectification probe which provides electron temperature, Te [Hirao and Oyama,1970] and an impedance probe for electron density, Ne [Oyma et al., 1986]. As these probes, especially, Te probe, have been flowing a number of sounding rockets and satellites, their performance is well established [Oyama et al., 2008]. Data was accumulated for 16 months, until the satellite operation was terminated in June 1982 due to the battery problem. The instruments gave accurate and reliable data in the ambient ionosphere plasma density Ne of $>10^4$ electrons /cc, and of Teup to 3000 K, with the accuracy of more than 10 %.

Figure 1 shows a model of The constructed by using data acquired by Hinotori launched in 1981. For all three seasons (northern summer, northern winter, and equinox), Te takes the minimum value at ~4 LT, rises steeply and shows a peak at ~9 LT (named as "morning overshoot"). After the morning over shoot, Te reduces toward noon, starts increasing at~15LT, and shows the second peak at ~ 17 LT (named as "afternoon overshoot"). Finally the peak disappears at around 20 LT. The first peak is not so sensitive to geomagnetic latitude, compared to the second peak. The second peak shows a clear latitudinal variation; the peak is not remarkable over the equator, but becomes clearer in higher latitudes.

Special Issue IJEAR Vol. 11 No 2 : **February 2025**

Proceedings of International Conference on Electronics and Advances in Science & Technology, (IConEAST-24)

Nov. 8-9, 2024

Towards mitigating natural hazards for a better humanosphere

Venue : Gauhati University, India

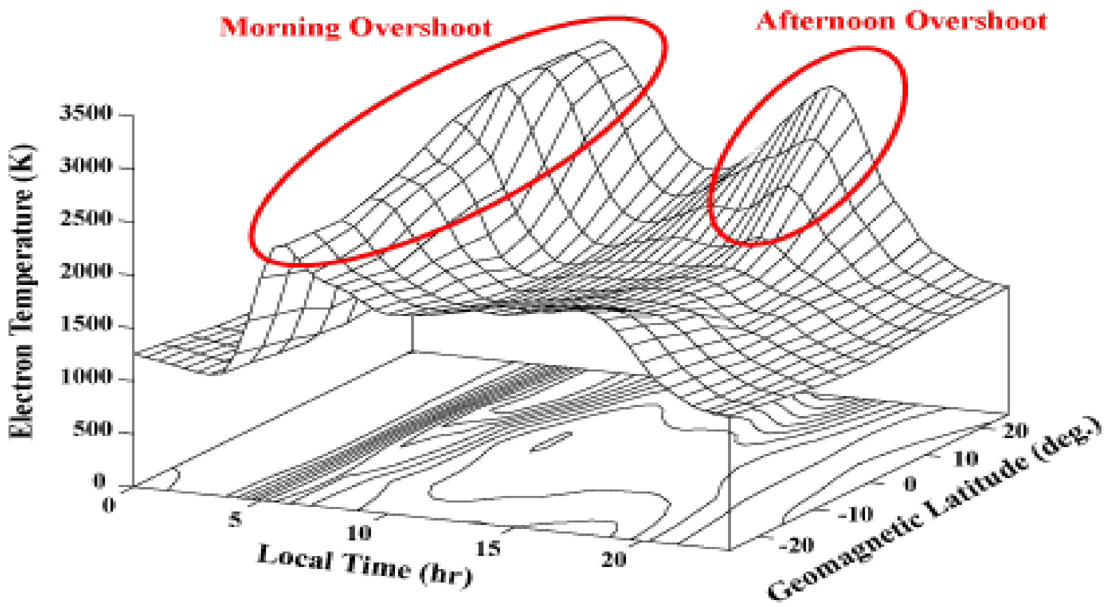

Figure 1: Local and latitude variation of Te observed by Hinotori satellite, a case for summer season in the northern latitude (Oyama et al., J. Geophys. Res, 2008).

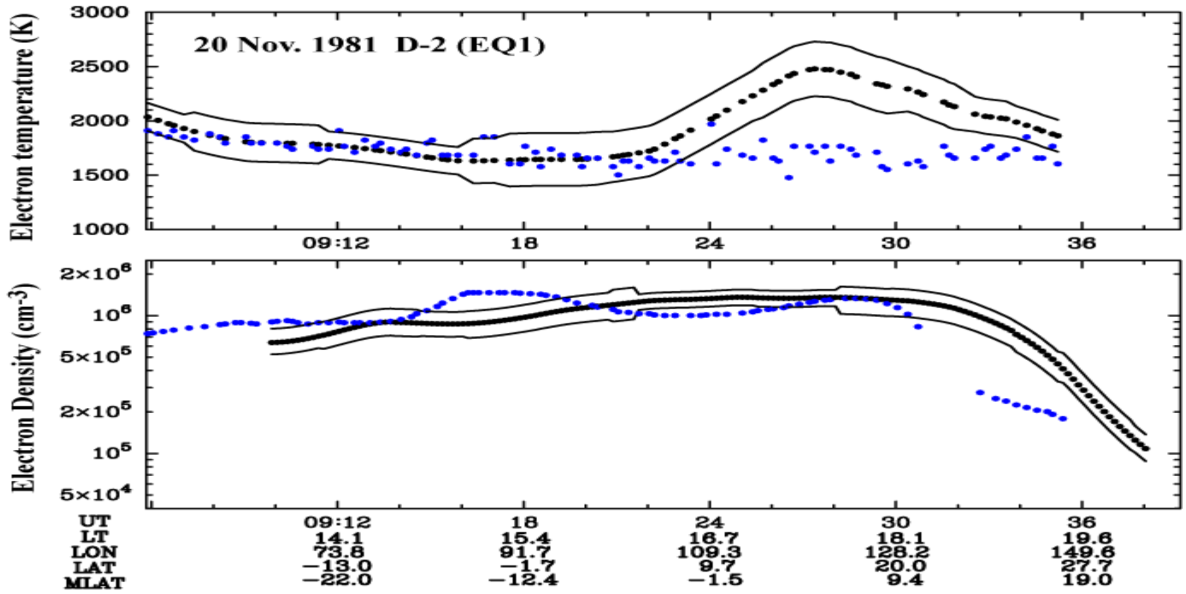

(a)

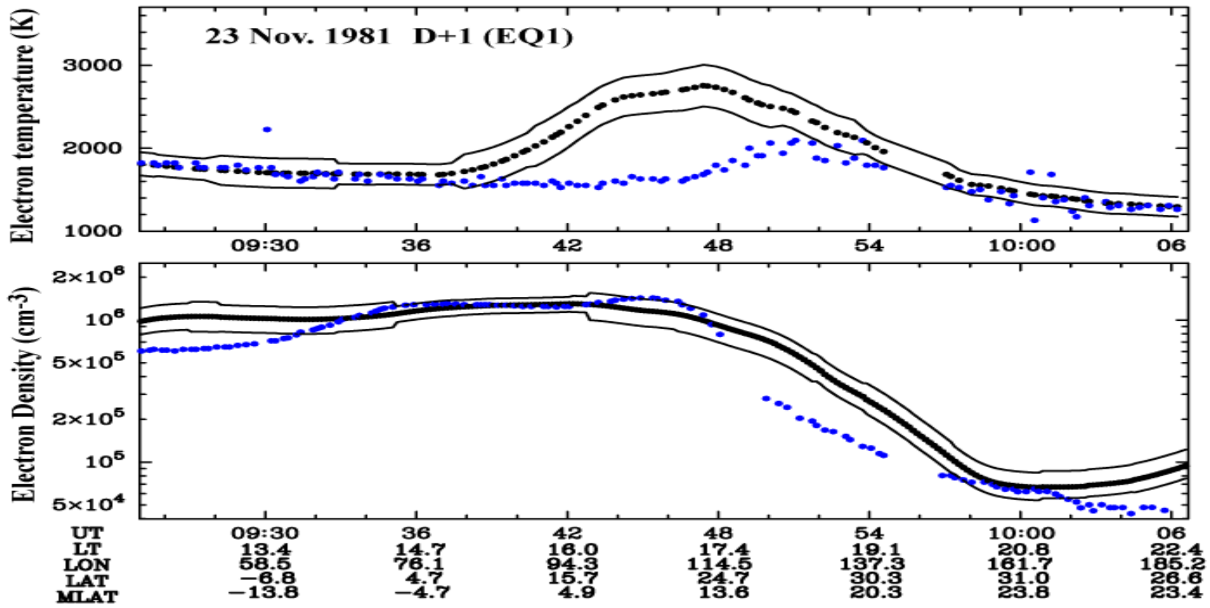

(b)

Figure 2: Total (a) and partial (b) disappearance of the afternoon-overshoot of Te, (upper) and Ne (lower), which was observed on 20 November, 1981, 2 days before the EQ. 3 days later i.e., after the event, total disappearance of Te changes to the partial disappearing. The dotted black line is Te, as shown in Figure .1. The blue dotted line is Te observed on 20 November 1981 for EQ 1. The thin curves are the standard deviation for both Te and Ne (Oyama et al., J. Geophys. Res, 2008).

By using the data acquired by Hinotori we studied three earthquakes which occurred in the north of the Republic of the Philippines [Oyama et al., 2008]. These are the earthquakes (EQ1) occurred on 22 November 1981 With magnitude Ms of 6.7, depth of 37 km, the epicenter of 15.05°N and 120.84° E. Other two earthquakes are ; (EQ2) of 1982/1/11,with epicenter at 13.75°N,124.36° E, depth 45km and magnitude Ms= 7.4, and (EQ3) of 1982/1/24, with epicenter at 14.09°N, 124.35° E ,depth 37 km , and magnitude Ms=6.6. Figure 2(a) shows total disappearance of the afternoon overshoot of Te, 2 days (blue dotted line) before the earthquake of November 22 , 1981 (displayed for one of 3 earthquakes) .and partial restoration of the same after the event (Figure 2b). We did not understand the physics of the behavior of Te for these earthquakes at the beginning. Usually it is seen that when Ne reduces, Te increases during daytime. While in this case, the afternoon overshoot of Te disappears without the changes in Ne. The behavior of Te can be explained as follows: below

600 km, increase of Ne occurs due to the poleward shift of equatorial ionization which is caused by the enhanced dynamo electric field. While photoelectrons pass through the dense plasma region caused by the poleward shift of the high density region, the energy is dissipated among the high electron density region.

1b. O^+ Density Measurement

Reduction of O^+ density was observed by Dynamic Explorer-2 (DE-2) satellite before three earthquakes which occurred near Chile in 1981. The DE-2 had an eccentric orbit of ~1000 km as apogee height /~300 km perigee height. Around the perigee height, the O^+ density starts the reduction about 5 days before the earthquakes, shows the minimum on the earthquake days, and goes back to the normal after the earthquake. *The data shows that we can identify the date of the earthquake and the epicenter if the satellite orbit is lower than 300 km, where plasma structure is still not influenced by neutral wind and electric field.*

O^+ density data observed by the US satellite, DMSP F15 was also used to study the ionosphere modification during the preparation period of the earthquake which occurred on 11 March 2011 in Japan. The orbit altitude was about 800km, the data shows three following special behaviors:

1. Equator-ward shift of mid-latitude trough before the earthquake, the lowest latitude on the earthquake days, and returns to the original latitude.
2. Small increase of O^+ density at the north of the epicenter.
3. The increase of O^+ density over the geomagnetic equator.

1c. Special care for the instruments

It should be noted that TeNeP is only instrument which can measure Ne and Te, accurately, when we prepare for the earthquake satellite mission which consists of Cube-sats, and small satellite [Oyama et al, 2012; Oyama et al., 2015].Retarding potential analyzer and Plasma drift meter, need special attention to remove the electrode contamination. Topside sounder is needed to measure the height profile to check the height profile of plasma density calculated by using TEC tomography method.

Finally, my conclusion is that this presentation is prepared to encourage people to get interested in the precursor phenomena, and to start the ground-based data analysis as a first step, and work together for satellite constellations especially among earthquake suffering countries.

2. Acknowledgements

The content of the presentation is contributed by; C. H. Chen, Y. Sun, H. K. Juang, U. Das, K. Ryu, M. Devi, L. Bankov, J.Y. Liu, H. Liu, T. Kodama,, M. A. Abdu, Y. Kakinami, M. Kamogawa, C. Y. Chen, H. Fang, T. Uozumi, I. Kutiev and N. Ishii.

The research was partly supported by Mitsubishi Foundation in 2014.

References

Bankov, L. G, S. M. Belyayev, V .I. Ionova, G.V. Lizunov, O.G. Melanchenko, and K.-I. Oyama, (2017) Space mission "CLUSTERION": investigation of the dynamical processes in the ionosphere using a cluster of "YUZHSAT" satellites, *Space Sci. & Technol*. 233, (6), 25-33.
https://doi.org/10.15407/knit2017.06.025,2017.

Chen, C. H., K.-I. Oyama, H. K. Jhuang, and U. Das, (2023) Driving Source of Change for Ionosphere before Large Earthquake -Vertical Ground Motion-, *Remote Sensing, 15(18), 4556.*
https://doi.org/10.3390/rs15184556.

Chmyrev, V., A. Smith, D. Kataria, B. Nesterov, C. Owen, P. Sammonds, V. Sorokin, F. Vallianatos, (2013) Detection and monitoring of earthquake precursors: Twin Sat, a Russia–UK satellite project, *Adv. in Space Res.*,52,1135–1145.

Hirao, K., and K.-I. Oyama (1970), An improved type of electron temperature probe, *J.Geomag. Geoelectr.* 22, 393-402.

Jason S., S. Pulinets, A. S. Curiel, and S. Liddel, (2002) Earthquake Science Research with a microsatellite,10.1098/rsta.,1119, *Royal Soc*. London.

Korepanov, V., G. Lizunov, O. Fedorov, Yu. Yampolsky, and V. Ivchenjo, (2008) IONOSAT-Ionospheric satellite cluster, *Advances in Space Research*, 42.1515-1522.

Oyama, K**.-I.,** and K. Hirao, (1975)Erroneous evaluation of electron and ion temperature from a contaminated retarding potential trap, *Planet. Space Sci.,* 23, 1309-1312.

Oyama K.-I.,K. Hirao,T.Takahashi,and S.Watanabe, (1986) Observation of low latitude ionosphere by the impedance probe on board the Hinotori satellite, *J. Geomag. Geoelectr.*, 38,111-123, https//doi.org/10.5636/jgg.38.111.

Oyama,K. I., C. H. Lee, H. K. Fang, and C. Z. Cheng, (2012) Means to remove electrode contamination effect of Langmuir probe measurement in space, *Rev. Sci. Instrum.*, , 83(5):055113, doi:10.1063/1.4722167.

Oyama, K. I.,Y.W. Hsu, G. S. Jiang, W. H. Chen,C. Z.Chen, H. K. Fang, and W.T. Liu, (2015), Electron temperature and density probe for small aeronomy satellites, *Rev.Sci.Instrum*.,86, 084703, doi:10.1063/4927342

Oyama,K.-I**.**, Y. Kakinami, J. Y. Liu, M. Kamogawa, and T. Kodama, (2008) Reduction of electron temperature in low latitude ionosphere at 600km before and after large earthquakes, *J.Geophys.Res*., doi:10.1029/2008JA013367.

Oyama, K. -I., Y. Kakinami, J.Y. Liu, T. Kodama, and C.Y. Chen, (2010), Micro/mini satellites for earthquake studies - toward international collaboration, *Advances in Geoscience*, 21, 251- 256.

Oyama, K.-I., Y. Kakinami, J. Y. Liu, M. A. Abdu, and C. Z. Cheng, (2011), Anomalous Ion Density Latitudinal Distribution as a precursor of large earthquake, *J. Geophys. Res.*, 116, A04319, doi:10.1029/2010JA015948.

Oyama, K. I.,and M. Devi,(2020) Study of Anomalous behavior of ionosphere prior to large earth quakes - Present and Future, *Space Res. Today*, 2020 August Issue, No 208, 36- 43.

Oyama, K., C. H.Chen, and M. Devi, Model of the electric field generation to modify the ionosphere, under preparation.

Picozza, P,L. Contiand,and A.Sotgiu, (2021) Looking for Earthquake Precursors From Space:

A Critical Review, *Frontiers in Earth Science*,doi:10.3389/feart.2021.676775,

Sun, Y.Y., K. -I. Oyama, J. Y. Liu, H. K. Jhuang, and C.Z.Cheng,(2011) The Neutral Temperature in the Ionospheric Dynamo Region and the Relation with the Ionospheric Density duringWenchuan and Pingtung Earthquakes, *Nat, Hazard. Earth Syst. Sci*., 11, 1759-1768.

About the author and keynote speaker

.

e-mail: ichiro@yahoo.ci.jp

Prof. Koichiro Oyama devoted his whole life to ionosphere study at the same space Research organizations(the Institute of Space and Astronautical Science (ISAS), University of Tokyo (UTK), then separated from UTK, then later merged with Japan Space Exploration Agency (JAXA) until he retired in March 2006. Then he was invited by National Central University, Taiwan, and then by National Cheng Kung University. Before he retired from ISAS, he engaged in the measurement of electron temperature in the ionosphere by using sounding rockets not only inside Japan but also outside Japan such as India, the USA, Brazil, and West Germany. The probe was accommodated in the following earth-orbiting satellites; 1975 Taiyo, 1978 Kyokko, 1981 Hinotori, and 1985 Ohzora. The energy distribution of thermal electrons up to 8000 km was measured by Akebono which was launched in 1989. In 1986 He was engaged in solar wind measurement and accommodated 1^{st} Japanese interplanetary spacecraft Sakigake during the Halley comet International campaign. He was a contact point of Japan for the Dynamics Adapted Network (DYANA) proposed by Prof . Offermann in 1988-1989. Until 1989 he worked as a test conductor of many sounding rockets as well as balloon experiments.

His final task at ISAS was to propose the Venus orbiter(named AKATSUKI after the launch) mission as Working Group Chair. In parallel with his academic work, he spent time on space Education. He was a co-chair of the space education working group under the umbrella of the Asia-Pacific Space Agency Forum and started Water boosted Rocket Competition among Asian countries. Since 2019 he is the president of the Satellite Design Contest in Japan organized by 5 academic societies. Currently, he is doing research on the abnormal behavior of the ionosphere before large earthquakes.

Special Issue IJEAR Vol. 11 No 2 : **February 2025**

Proceedings of International Conference on Electronics and Advances in Science & Technology, (IConEAST-24)

Nov. 8-9, 2024

Towards mitigating natural hazards for a better humanosphere

Venue : Gauhati University, India

Anomalous variations of the pH parameter of the underground thermo-mineral waters as possible earthquake precursors

Farshed H. Karimov*, Shodruz A. Olimov, Bahrom A. Olimov

Institute of Geology, Earthquake Engineering and Seismology of the National Academy of Sciences of Tajikistan Tajikistan

Article History : *1st received: 20.12.2024 Final : 27.1.2025*

Abstract:

The paper presents the variation of pH parameter in the self-flowing out wells of underground thermal mineral water deposits in Southern Tajikistan Obigarm, Khoja-Obigarm, Shaambary and Yavrozon the territory of Tajikistan in association with strong earthquake and on the development of methods for the identification of tectonic earthquakes precursors. The Observation sites are in the vicinity of large active seismogenic zones, where anomalies in pH parameters are expected, reflecting the processes of an earthquake source preparation. The empirical spatial-temporal patterns of the seismotectonic cycle and theoretical models of the processes of preparation of tectonic earthquakes are adopted, taking into account the size of the preparation area and the source along with the duration of long-term anomalies' manifestation and their dependencies of magnitude.

Part of the keynote speech delivered by Dr. F H Karimov at the International Conference on Electronics and Advances in Science & Technology (IConEAST-24) held during Nov 8 and 9, 2024, at Gauhati University, Guwahati India. fhkarim85@gmail.com

1. Introduction

According to standard concepts, hydrodynamic, hydrological and hydrogeological studies, which are devoted to the study of seismotectonic processes based on observations of the physicochemical parameters of underground waters, are called seismo hydrogeochemical.

ISSN: 2395-0064

The experience of observing variations in hydrogeological and hydrogeochemical parameters of underground thermo-mineral waters in seismically active areas, in particular in Tajikistan, makes it possible to identify a number of features in their temporal course: trends, periodicities and anomalous variations [Karimov et al., 2017]. If we compare these features with the well-known concepts of the development of seismotectonic cycles [Sadovsky, 1987] as states of the geomedium in the time intervals between earthquakes of the highest magnitudes with foci in a certain seismogenic cluster, then trends can be attributed to the regular state of the environment and the long-term stage of earthquake preparation [Dobrovolsky, 1991], periodicities to the action of lunar-solar tides [Abramov and Dolginov, 2013; Metivier et al., 2009] and atmospheric processes [Latynina and Vasiliev, 2001; Bykov, 2005], or seasonal changes in the state of groundwater [Kissin, 2009], local anomalous variations to the mid or short-term stages of earthquake preparation [Dobrovolsky, 1991], or to such local geodynamic phenomena as a seismic creep [Sadovsky,1987; Dobrovolsky, 1991], or subsidence in the soils of mountain ranges [Scheidegger, 1981]. Trends can also be observed at the post-seismic stage, at which the geotectonic stresses of the medium relax and its transition to a regular state occurs [Dobrovolsky, 1991]. According to estimates [Sadovsky,1987], the time interval of the long-term stage of preparation of tectonic earthquakes in the Central Asian region is about one tenth of the duration of the seismotectonic cycles.

The present work is devoted to the study of variations in one of the numerous hydrogeochemical parameters of underground thermo-mineral waters, namely the pH parameter, deposits in the settlements of Yavroz (1), Obigarm (2), Khoja-Obigarm (3), Shaambary and (4) in Tajikistan (Figure 1).

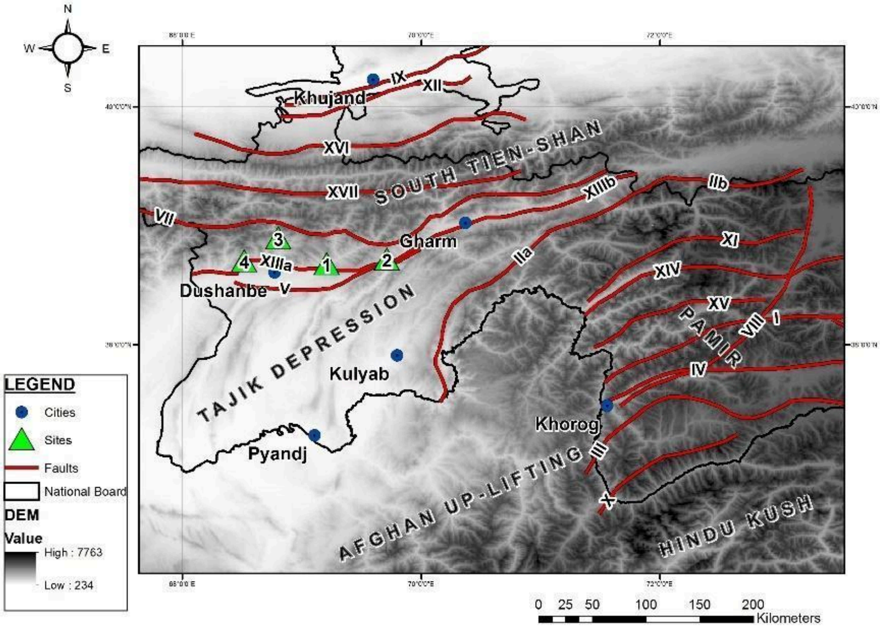

Figure 1: Geostructures of the observational area and the layout of the seismic geochemical sites.

2. Organization of seismic geochemical observations

Tajikistan covers the geostructures of the Tajik Depression and the Southern Tien Shan, the southern slope of the Gissar Range, and the southwestern part of the Karategin Range. The Tajik depression is composed of Meso-Cenozoic sediments up to about 10 km thick above the crystalline basement. The relief here is contrasting with local depressions replaced by mountain rises. Salt complexes are widespread. The geostructures of the Southern Tien Shan are a highly elevated Paleozoic massif composed of block structures with synclinal bends between them [Baratovet al., 1981; Fusailov and Musin, 1982]. The Moho boundary runs at depths of 40-50 km [Baratovet al., 1981; Fusailov and Musin, 1982; Gubin and Zakharov, 1983]. All these stations are located in the vicinity of large active faults in the Earth's crust (numbered with Roman numerals in the Figure. 1): Yavroz, Obigarm, Shaambary on Gissaro-Kokshaal (Southern-Gissar) of the 1st order with the earthquakes' magnitude (M) up to 7.5 and Ilyak-Vaksh of the 2nd order with M up to 6.5, and Khoja-Obigarm on

Karakul-Pitaukul with M up to 6.5 [Karimov et al. 2017; Gubin 1960 ; Babaev and Mirzoev 1976 ; Mirzoev 1982 ; Lukk and Junga 1988 ; Burtman 2013], which can generate earthquakes with intensities up to 8-9 points on the MSK scale [Medvedev et al., 1965]. Elevation on Figure 1 marks the range above sea level from a maximum of 7763 m (high) to a minimum of 234 m (low).

3. Brief description of the hydro-geochemical structure of the observation-site

Studies of the geological structure of the observation area show that it is subject to active geotectonic, geodynamic, seismic and hydrogeochemical processes, there are relatively high rates of tectonic movements of the Earth's crust, amounting to 1 cm/year in the order of magnitude [Lukk and Junga, 1988 ; Burtman, 2013 ; Ishchuk et al., 2013], there are explosion tubes [Baratovet al., 1981; Fusailov and Musin, 1982], indicating active orogeny in the past. The geological activity of the research area is also evidenced by the relatively high density of the heat flow of the earth's crust. In the pre-Gissar trough, in the zone of the South Gissar deep fault, it increases from east to west, reaching 100.4 mW/m^2 in the area of the Shaambary anticline [Baratovet al., 1981 ; Fusailov and Musin, 1982]. The average heat flow of the Tajik depression is 62 mW/m^2. Temperatures at a depth of 1000 m below sea level in the area of Yavroz is 76^0 C, Obigarm is 70^0 C, Shaambary is 70^0 C, Khoja-Obigarm is 90^0 C and more [Fusailov and Musin, 1982]. According to the temperatures of the subsurface, the temperatures of underground thermal and mineral waters are relatively high: below about 40^0 C in Yavroz, Obigarm and Shaambary, and above about 90^0C in Khoja-Obigarm (Table 1). Such values of water temperature indicate the depth of their circulation up to several km, which is commensurate with the depths of the foci and crustal earthquake preparation zones in the observation area. Since temperature in the Earth's interior are directly related to geotectonic and seismotectonic processes, it is reasonable to expect that the pH parameter in the groundwater of the research area may directly indicate activation, or, conversely, a lull in the development of these processes. In particular, it is known that as the temperature of water increases, its pH usually increases [Todt, 1967]. Therefore, temperature changes in the Earth's interior reflecting geotectonic and seismotectonic processes, along with changes in porosity and humidity of the medium, which determine the interaction between solid and fluid phases, may be the direct causes of variations in the pH of underground thermo-mineral waters.

Data on the depths of wells for water extraction, their average temperatures, flow rate and chemical types, which are important in determining physics-chemical and, in particular, seismo-geochemical parameters, are given in Table 1.

Table 1: Physical-chemical characteristics of ground water.

№	Location φ,^{0N}λ, ^{0E}	Wells' depth, (absolute heights), m	Mean temperature, ^{0}C	Mean debit, l/c	Kind of waters
1	Yavroz 38.68 69.21	271.8 (1111)	45	0.4	Chloride-Sulfate -Sodium
2	Obigarm 38.72 69.71	630 (1287)	45	2.5	Sulfate-Chloride -Sodium
3	Khodja-Obi garm 38.90 68.80	46.5 (1780)	63	1.2	Bicarbonate-Sulfate-Chloride -Sodium-Siliceous
4	Shaambary 38.63 68.62	1377 (1202)	39	1.3	Chloride-Sulfate -Sodium

The preparation areas for tectonic earthquakes with M ≥ 4 cover depths of up to tens or hundreds of kilometers of the Earth's interior [Sadovsky 1,987 ; Dobrovolsky, 1991; Metivier et al., 2009], and therefore fluids can contribute to the development of seismotectonic cycles. However, field observations and field & laboratory experiments show, that the degree of this contribution can vary from low, [Sadovsky, 1987], for example, in the Avalanche Growing

Cracks (LNT) model [Myachkin et al., 1975], to high, for example in the dilatation diffusion model (DD) [Nur, 1972 ; Anderson and Whitcomb, 1973]. In a number of models of earthquake formation foci, both fluid and non-fluid processes turn out to be important at the same time, for example, in the model of abrupt slip along a ready-made rupture [Dietrich, 1977], friction significantly depends on humidity at the boundary of the contacting blocks. More generally, the importance of the hydro-geochemical studies under consideration is determined by the fact that studies, in particular of the pH parameter, in addition to detecting earthquake precursors, can lead to the definition of indirect criteria for assessing the role of fluids in specific seismo-tectonic processes [Kissin, 2009].

4. Methodology for determining and identifying abnormal variations in the pH parameter

The pH value is one of the most important indicators of the properties and quality of waters and characterizes the state of acid-base equilibrium in them. A pH value above 7 usually indicates alkalinity and below 7 indicates acidity. In pure water at a temperature of 22^0C, the concentration of hydrogen ions ($[H^+]$) and hydroxyl ions ($[OH^-]$) is the same and amounts to 10^{-7} mol/l. The pH value equal 7 indicates the neutral solution, pH > 7 a base and pH < 7 an acidity. Since the rock features (cracks, porosity and pore surface area) change during seismic cycles, the pH of thermal mineral waters also changes, and therefore it can be expected that changes in the pH parameter will reflect the earthquake preparation process.

Water sampling and measurements were carried out using standard methods to pour from self-draining wells into glass bottles. The nominal measurement accuracy of the pH parameter was 0.01 pH units. In parallel, the temperature of water and atmospheric air, as well as of atmospheric pressure, was measured. Methodologically, the determination of anomalies in variations in the pH parameter of underground thermo-mineral waters is based on solving direct and reverse geophysical problems for the area of location of seismo-geochemical sites. The solution to the direct geophysical problems consisted in determining potential pH trends and anomalies from known earthquake sources based on known empirical and analytical dependencies. The solution to the inverse problems was to establish the correspondence of the detected pH anomalies to the seismo-tectonic cycles of the formation of specific earthquake foci. The consideration in this paper is based on the idea of the geophysical environment as having a continuum-discrete structure, hierarchically composed by geo-blocks of different scales, separated by boundaries of various types from micro level from dislocations and cleavage in rock minerals, to the macro level of cracks in rocks, ruptures and faults in the Earth's crust, and to mega levels of deep faults of the lithosphere and lineaments in tectonic plates boundaries [Sadovsky,1987 ; Sadovsky,1984]. Accordingly, the hierarchy of the lithosphere structure determines the hierarchy of stresses in it during deformation processes occurring with or without disturbances in the continuity of medium. Seismological observations and model estimations show that the linear sizes and volumes of tectonic earthquake foci as sources of seismic wave radiation in the hierarchy of geo-blocks directly relate to the scale of fault zones and are proportional to magnitudes [Sadovsky,1987 ; Sadovsky,1984]. Expressions are known for the maximum linear dimensions of the foci in the direction along the displacement along the fault and across to it, respectively [Riznichenko,1976]:

$$\log log\, L\ [km] = 0.44\ M\text{-}1.29, \quad (1)$$

$$\log log\, l\ \ [km] = 0.40\ M\text{-}1.45, \quad (2)$$

Where, L and l are, respectively, the major and minor axes of the ellipsoid.

Expressions (1) and (2), as the average approximate logarithmic dependences, according to Riznichenko, [1976], these are valid for a wide range of M from -2 to 9. However, it should be borne in mind that the use of expressions (1), (2) is limited by the magnitude and depth of the hypocenter, since, for example, for the severe earthquakes, the size of the foci significantly exceeds the thickness of the earth's crust and therefore can be applied with a certain degree of conditionality. Indeed, according to (1),(2), for example, for M=7, the average size of the hearth is 40 km, for M=8 is 100 km, for M=9 is 260 km. To analyze variations in the pH parameter of underground thermo-mineral waters based on known empirical analytical dependencies for the characteristics of the geophysical environment [Sadovsky,1987 ; Dobrovolsky, 1991; Sadovsky,1984] and models of the seismotectonic cycle [Sadovsky,1987; Dobrovolsky, 1991;Myachkin et al, 19751; Nur, 1972; Anderson and Whitcomb, 1973, ; Dietrich, 1977 ; Sadovsky,1984], three types of epicentral zones can be distinguished, in which the corresponding features of the manifestation of variations in the pH of a seismotectonic nature are expected: the near, occupying the volume of the forming hearth earthquakes [Sadovsky,1987; Dobrovolsky, 1991;Myachkin et al, 1975; Nur,1972; Anderson and Whitcomb, 1973 ; Dietrich, 1977; Sadovsky,1984; Riznichenko,1976], the average, to the margin of which the relative strains of the geomedium decrease to background values of 10^{-8} [Dobrovolsky, 1991], determined by lunar-solar tides [Abramov and Dolginov, 2013; Metivier et al., 2009], and the far, its existence is caused by the passage of large fault zones and, apparently, precisely because of the relatively high porosity of rocks in zones of large tectonic faults, seismogeochemical anomalies can manifest themselves anisotropically in the directions of the lengths of these zones at distances up to 1000 km, much exceeding the size of foci and preparation zones [Sadovsky,1984]. This separation of the features of the expected pH anomalies in these three epicentral zones is justified, in particular, by differences in the nature of environmental strains within and outside the focal zone (see, for example, [Dobrovolsky, 1991]). The linear dimensions of the near zone, as a focal zone, are described in the first approximation using expressions (1) and (2), the average in which the focus is formed and the stresses decrease to the background, according to analytical estimates in the approximation of a spherically symmetrical focus with a radius of *R* as follows –

$$\lg R[\mathrm{km}] = 0.43\ \mathrm{M}. \qquad (3)$$

According to the current experience of detecting geophysical anomalies accompanying earthquake preparation [Sadovsky,1987; Dobrovolsky, 1991], there are three-time stages, such as long-term, medium-term and short-term [Sadovsky,1987; Dobrovolsky, 1991; Sadovsky,1984], and since the dynamics of groundwater depends on strains of their host environment, it can be expected that hydrogeochemical anomalies corresponding to these stages, will be detected along with the time. As noted at the beginning of this article, the long-term stage of earthquake preparation is approximately one tenth of the duration of their seismotectonic cycles [Sadovsky,1987; Sadovsky,1984]. The latter depends on the magnitude, the activity of geotectonic processes, and the thickness and structure of the geological structures in which the foci is formed. For example, in the western sub district of the Gissar-Kokshaal fault in the observation area, to the west of Fayzabad stage, the recurrence of earthquakes with a maximum energy class of K=17 (M=7.2) is 1400 years, with K=16 (M=6.7) is 500, K=15 (M=6.1) is 200 and for the eastern sub district for K=18 (M=7.8) is 160 years, for K=17 (M=7.2) is 55, for K=16 (M=6.7) is 20 years, for K=15 (M=6.1) is 7 years [Gubin,1960 ; Babaev and Mirzoev,1976 ; Mirzoev,1982]. It is very difficult to practically trace the beginning of the long-term preparation stage due to the limited observation time, especially for large-magnitude earthquakes. Under the influence of gravity and constant pressure of the Indian Plate on the Eurasian plate, the observation area is subject to background strains of the lithosphere compression. Data from the global positioning of the earth's surface convincingly show that as a result of the subduction of the Indian Plate under the Eurasian Plate [Lukk and Junga, 1988 ; Burtman, 2013; Ishchuk et al., 2013]constant unidirectional tectonic stresses act on the observation area and it is subject to deformations on a scale of about 1000 km. This background pattern of stresses and strains is overlaid by deformation waves [Gorbunova and Sherman, 2012], especially from major earthquakes occurring in the region. The possible seismic effect of the propagation of deformation waves over distances of thousands of km and their passage through the territory of Tajikistan was considered in the case [Karimov, 2020], using the example of a mega earthquake with an epicenter on Sumatra Island on 26.12.2004 with M=9.2.

ISSN: 2395-0064

The propagation of deformation waves from large earthquakes with M ≥ 7 can also be evidenced by the generation of large crustal earthquakes by Hindu Kush deep-focus earthquakes in Tajikistan with lags from a month to a year [Katok,1991], as well as grouping [Mirzoev and Azizova, 1982], clustering [Smirnov and Ponomarev, 2020], migration of earthquake foci [Kulagin and Halimova, 1982], foreshock and aftershock activity [Pshennikov, 1965]. On the sections of the borders of some adjacent geoblocks moving at different speeds, due to the "hook" between them, their local deceleration occurs when the deformation energy of the surrounding geoblocks is pumped here, when a heterogeneity forms and grows, in which an inclusion will subsequently form a prototype of the prepared foci [Dobrovolsky, 1991]. This is the beginning of a long-term preparation stage, which is characterized by anomalous deformations of the Earth's crust in the form of a trend. The areas of preparation for at least earthquakes with M≥4, according to estimates according to (Dobrovolsky, 1991), cover two adjacent or more geoblocks of the earth's crust. With the onset of switching on, the stresses begin to concentrate mainly in the vicinity of some adjacent blocks, between which the most intense energy "hook" has occurred, switching on in its vicinity, and the mid-term preparation stage begins. The inclusion, in fact, is a stress concentrator, similar to the one known in the mechanics of fracture of solids [Pshennikov, 1965; Kuksenko,1984], which is the prototype of a future earthquake source. In the initial phase, due to the pumping of energy from the outside, there is an increase in stresses in the area of heterogeneity and plastic compression of the inclusion medium. Further, with increasing stresses in the inclusion, discontinuous disturbances of the medium from the crack hierarchies appear in terms of the LNT and DD models [Dobrovolsky, 1991; Myachkin et al., 1975; Nur,1972; Anderson and Whitcomb, 1973; Dietrich, 1977]. Further, in accordance with the theory of preparation of a tectonic earthquake [Dobrovolsky, 1991], a zone weakened by cracks grows in the inclusion and its transition to a critical, unstable state, during which a short-term stage develops, up to rapid movement at the time of the earthquake.

In accordance with the data presented on the seismotectonic cycle, we present a model of the dynamics of variations in the pH parameter at the stages of the regular state (1), long-term, mid-term, short-term (2), and post-seismic (3) in the form of a time course with a bay-shaped anomaly (Figure 2). The moment of the earthquake is indicated by the magnitude arrow M. Depending on the chemical type of groundwater, pH variations in them in seismotectonic cycles can obviously be relative to the regular state 1 as positive (marked with solid lines) and negative (dotted lines). The greater the magnitude of the impending earthquake, the more intense, earlier, and in a larger area the anomalies should appear.

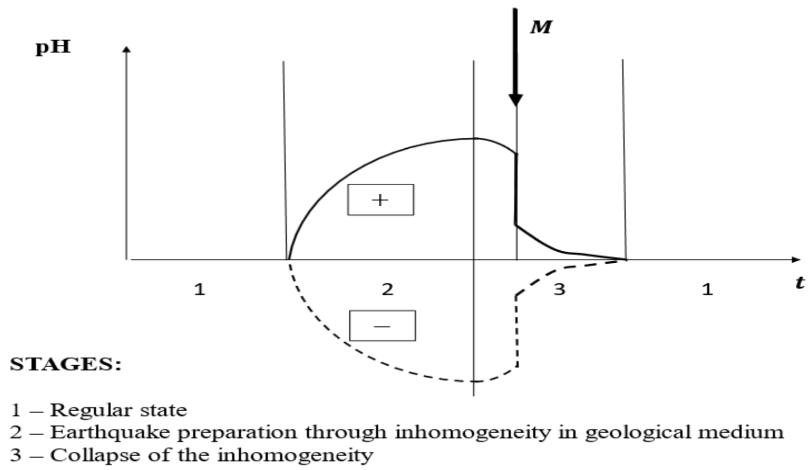

Figure 2: Bay-like expected shape of the pH anomalous variations in the underground thermal mineral waters.

So, the largest linear dimensions of the medium at the long-term stage of preparation are described using expression (3), and in the medium and short term stages are by equations (1) and (2), respectively .By averaging (1) and (2), an expression is obtained for the average linear size of the inclusion, D_0,

$$\log log\ D_0[km] = 0.413M - 1.397. \tag{4}$$

Special Issue IJEAR Vol. 11 No 2 : **February 2025**

Proceedings of International Conference on Electronics and Advances in Science & Technology, (IConEAST-24)

Nov. 8-9, 2024

Towards mitigating natural hazards for a better humanosphere

Venue : Gauhati University, India

Table 2 provides summary data on the linear sizes of the zones of long-term, D, (3), mid-term, D_0, (4), anomalies in the strain of the Earth's crust. Since the sources of short-term anomalies in the strains of the Earth's crust, according to theory [Dobrovolsky, 1991], are located in the zone of formation of the foci, i.e. inclusions, it is natural to expect that they can be most clearly detected in this zone with linear dimensions of the order of foci itself,D_0, where the stresses are greatest. Table 2 shows the linear dimensions of the inhomogeneity and inclusion zones.

Table 2: The linear dimensions of the in homogeneity and the inclusion zones.

M	3	4	5	6	7	8
D, km	40	100	280	760	2040	5400
D_0, km	0.68	1.79	4.66	12.05	31.19	80.7

According to [Dobrovolsky, 1989], the time of manifestation of anomalies in the strains of the Earth's crust at the long-term stage, at which the heterogeneity of the environment is formed and in which the inclusion of a future source will subsequently occur, is described using the expression

$$lg\Delta T_l\,[years] = 0.5M - 2.10. \qquad (5)$$

For the Mediterranean (similar to the Central Asian) region, the following formula was obtained for the time of manifestation of "deformation precursors" from the energy of the corresponding earthquake [Sadovsky,1987; Dobrovolsky and Zubkov,1989] (according to the time values, it can be seen that the expression describes the mid-term stage at which the inclusion, the embryo of the focus, is formed):

$$lg\Delta T_m[years] = 0.56M - 2.9. \quad (6)$$

For short-term precursors based on data on strains of the Earth's crust, the following empirical expression for the time of their manifestation is given in [Dobrovolsky, 1989]

$$lg\Delta T_s[years] = 0.26M - 3.50. \quad (7)$$

In [Sadovsky, 1984 ;Nikonov, 1977], basing on data from the classical theory of elasticity about decrease of mechanical strains in the stress concentration zone for solids [Salomov et al, 1982; Salomov et al., 1982a ; Panasyuk, 1968] , the linear sizes of zones of anomalous deformations of the Earth's crust are assumed to be 10-15 sizes of foci, which, however, are several times smaller than the sizes of areas of heterogeneity of the long-term stage as can be seen from the Table 2. To analyze the pH variations of underground thermo-mineral waters, we will use the models of the geophysical environment [Sadovsky,1987; Dobrovolsky, 1991; Sadovsky,1984] and the results are based on empirical observations According to the standard approach, mechanical stresses and strains of the medium are considered as primary, underlying the occurrence of other geophysical fields, the anomalies of which also have their own spatial and temporal characteristics. Therefore, for long-term changes in the groundwater level, which we will take as an indicator for the manifestation of pH anomalies, an empirical formula is proposed [Dobrovolsky, 1989] as:

$$lg\Delta T_{uw} = 0.34M - 2.21. \quad (8)$$

For long-term anomalies in the flow rate of underground sources debit [Dobrovolsky, 1989,36] is given as:

$$lg\Delta T_{wd} = 0.23M - 1.38. \quad (9)$$

In accordance with expressions (5)-(9), Table 3 shows the values of the duration of long-, medium- and short-term anomalies in the strains of the Earth's crust, the duration of anomalies in groundwater levels and flow rates. For comparison, the last line contains data on short-term anomalies in the radon gas content in underground fluids [Dobrovolsky, 1989].

Table 3: Duration of seismogenic anomalies for strains of the Earth's crust and groundwater

M	3	4	5	6	7	8
$\Delta T_l, years$ (y.)	0.25 (91)	0.79 (288)	2.50	8.00	25.10	79.40
$\Delta T_m, y\ (days)$	0.06 (22)	0.20 (73)	0.79 (288)	2.90	10.47	38.02
$\Delta T_s,\ (days)$	0.73 (266)	1.10	2.20	4.02	7.30	13.85
$\Delta T_{uw}, y$ (days)	0.06 (22)	0.14 (51)	0.30 (110)	0.68 (250)	1.50	3.24
$\Delta T_{wd}, y\ (days)$	0.20 (73)	0.35 (128)	0.59 (215)	1.00 (365)	1.70	2.90
$\Delta T_{Rn}, y\ (days)$	0.003 (1)	0.004 (1.5)	0.006 (2.2)	0.01 (3.7)	0.016 (5.8)	0.025

Attention is drawn to the proximity of the durations of groundwater levels and groundwater discharge, which indicates a single mechanism of their origin. These durations are of the same order of magnitude as the mid-term durations of anomalous strains of the Earth's crust, rather than the long-term and short-term ones, ΔT_l and ΔT_m, respectively. Therefore, it can be assumed that the occurrence of detectable pH anomalies is based on the long-term preparation stage, at which, in accordance with the model of the geophysical environment adopted in this article, an inclusion is created, develops and disintegrates. Short-term anomalies in radon gas content give reason to believe that short-term pH anomalies, as well as other hydrogeochemical parameters of groundwater, will have similar durations (Table 3). Based on the known results of geotectonic, geodynamic, geophysical and seismological studies, we will adopt the following methodological approach to the identification and analysis of groundwater pH anomalies:

- Earthquakes are a rapid discharge of accumulated stresses in the Earth's interior caused by constantly occurring geo tectonic processes;

- Earthquakes are the fastest part of the development of the seismotectonic cycle in the time interval between the start of earthquake preparation and the processes of post-seismic relaxation;
- The regular state of the geological environment in seismically active areas is accompanied by the constant movement of geoblocks along fault zones under the influence of regional stresses from interacting tectonic lithospheric plates. In Central Asia, it is the Indian plate moving approximately in a northerly direction and the Eurasian plate, moving approximately in a southeasterly direction;
- The interaction of adjacent tectonic plates in Central Asia creates stresses on the boundaries between them and manifests itself in the form of subduction of the Indian Plate under the Eurasian Plate, crustal deformations, orogeny, formation of synclines and anticlines, development of lineaments and fault zones of different orders, and displacement of geoblocks and other lower-level structural units;
- The earthquake preparation stage begins with a violation of the regular geodynamic state of the geological environment, tectonic plates, geoblocks, and is characterized by a directional change in the stress state in the zones of passage of lineaments and faults of the Earth's crust;
- According to the theory of tectonic earthquake preparation [Dobrovolsky, 1991], regular friction, collisions, cohesion, and movements occur between adjacent geoblocks, that are in a stress-strain state, which manifest themselves, depending on their intensity, in microseisms and earthquakes;
- Excessive stresses accumulate at the junctions of adjacent geoblocks and foci of tectonic earthquakes form;
- The more intense, energetically secured coupling between adjacent geoblocks occurs, the more energy accumulates in the source;
- The accumulation of elastic and elastoplastic stresses in the hearth formation zone reaches critical values, after which the process of disintegration of this zone of

heterogeneity begins, first slowly, then quickly, ending in a violation of the continuity of the geological environment and earthquake movements, the stage of stress relaxation and transition up to a new regular state begins;

- The greater the accumulated energy, the greater the volume of the hearth, the area and the time of its preparation. The volume of the source and the preparation time depend logically on the magnitude of the earthquake;
- The stages of earthquake preparation are reflected in various stages of anomalous variations in geophysical fields: long-term, medium-term, short-term, and ultra-short-term. Since the groundwater is part of the phase and fluid composition of the Earth's crust and upper mantle, anomalies in variations in the pH parameter in deposits of underground thermo-mineral waters, the dynamics of which depends on geotectonic and geodynamic stresses, can manifest themselves at the stages of development of seismotectonic cycles;
- The greater the magnitude of the earthquake being prepared, the larger the area and over a longer period of time, anomalies appear in variations in geophysical fields and the pH of groundwater in particular;
- The bay-like nature of the time course of stresses in the hearth formation zone and the post- seismic stage should be reflected in the bay-like time courses of anomalies in variations in geophysical fields and the pH of groundwater, in particular.

5. Analysis of anomalies in pH parameter variations

Now, based on the ideas presented here about seismotectonic processes and models of the seismotectonic cycle, about the spatial and temporal characteristics of the manifestation of anomalies in the deformations of the Earth's crust at the long-, mid- and short-term stages of earthquake preparation, let’s try to establish a correspondence between the formation of their foci and anomalies in variations in the pH parameter of underground thermo-mineral waters. By solving direct geophysical problems from the list of possible earthquakes, the

ISSN: 2395-0064

seismotectonic cycles of which could manifest themselves in seismogeochemical anomalies, we will exclude in advance those of them that could not cause pH anomalies at the locations of seismogeochemical stations, and accordingly take into account only presentable ones that satisfy certain spatial and temporal dependencies and factors of anisotropy of fluid propagation along the fault zones (Tables 2, 3). Let's start the analysis with the strongest earthquakes from 2018-2019. Consider earthquakes with 7.5≤M≤8.0. According to dependences (3) and (4), the largest linear dimensions of the zone of manifestation of the corresponding pH anomalies should be within

$$R \leq 2750 \text{ km}, \quad (10)$$

and the average radius of the foci –

$$R_0 = 40,5 \text{ km}. \quad (11)$$

The duration of groundwater anomalies according to (8), (9) for earthquakes with M = 8 should be, respectively,

$$\Delta T_{uw} = 1181 \text{ days}, \quad (12)$$

$$\Delta T_{wd} = 1053 \text{ days}. \quad (13)$$

According to the catalog [USGS], since 2018, at an epicentral distance of up to 3,000 km from the network of seismic geochemical stations, there have been only two earthquakes with the highest magnitudes on the territory of Turkey i.e., on 6.02.2023 at 01:17:34 (UTC) with M=7.8, depth of 10 km., and on 6.02.2023 at 10:24:48 with M=7.5, the depth of the hearth is 7.4 km.

For the 1st earthquake, empirical expressions (8) and (9) give

$$R < 2260 \text{ km}, \quad (14)$$

and the average radius of the foci –

$$R_0 = 33.5 \text{ km}. \quad (15)$$

For the 2nd earthquake we have:

$$R \le 1680 \text{ km}, \tag{16}$$

and the average radius of the foci –

$$R_0 = 25.0 \text{ km}. \tag{17}$$

Firstly, the radii for the zones of possible pH anomalies (14), (16) for these two earthquakes are somewhat smaller than the epicentral distances of the seismogeochemical stations of about 3000 km. However, if we consider that two earthquakes occurred with an interval of about 9 hours, then we can conclude that the total magnitude exceeded 7.8 by tenths. Secondly, as seismogeochemical observations show, due to the anisotropy of the earth's crust caused, for example, by the passage of lineaments and fault zones, fluid filtration can extend over thousands of kilometers [Rikitake, 1983] and it can be assumed that the zones of manifestation of seismogeochemical and hydrogeological anomalies may exceed the empirical radii determined according to (8), (9). Thirdly, empirical dependences (12) and (13) were obtained as indicative and therefore are not universal for all seismically active areas. Indeed, such anisotropy may be due to the fact that a large seismotectonic belt passes through Turkey – the Alpine-Himalayan belt, which also passes through the territory of Tajikistan. This lineament includes an extensive network of crustal faults of various orders, from the 1st to the 3rd, and active fluid filtration can occur along them.

Therefore, we can expect corresponding anomalies in the pH variations of groundwater in the territory of Tajikistan during the seismotectonic earthquake cycle on 6.02.2023. Let's consider the course of the pH parameter according to the data of the Obigarm station, for which the most complete data were obtained for the period under observations since 2018 (Figure 3).

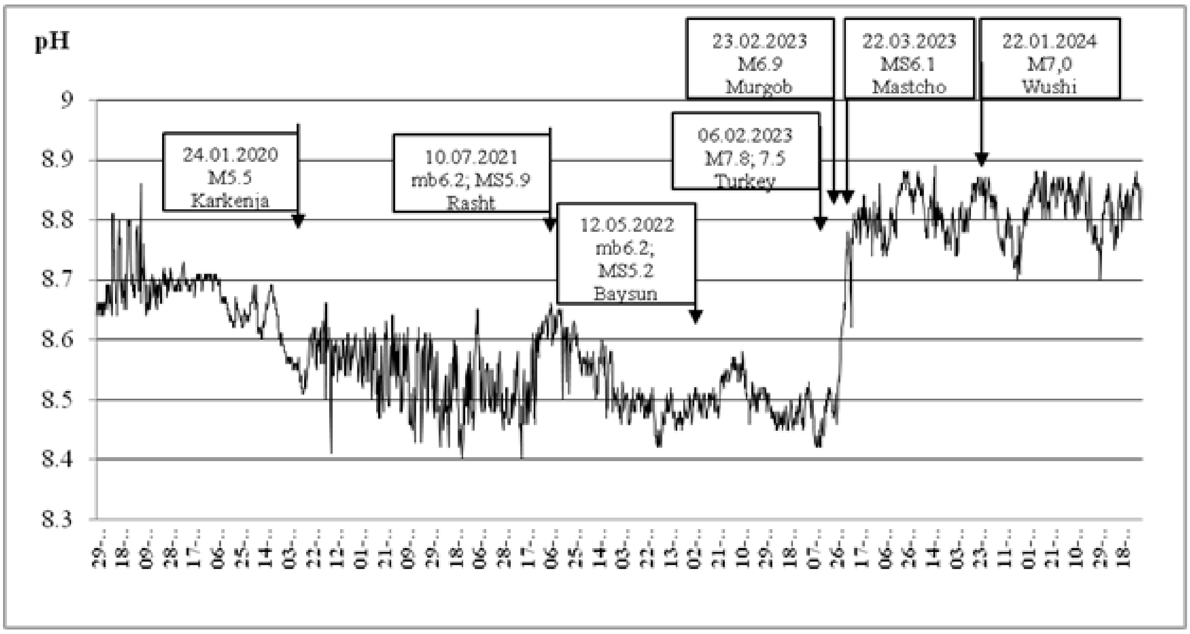

Figure 3: pH anomalies according to the Obigarm site data from 2019 to 2024 (dd.mm.yy).

The most recent of this series was the Wushi (Alkol) earthquake with M=7.0 on 22.01.2024 in China at epicentral distances to the observation network of about 1,900 km [Catalogues of Russian academy of sciences, the Geofon catalog, URL;Catalog of the American Geophysical Survey]. The spikes in the graphs reflect fluctuations in pH with a period of 1 day in order of magnitude, probably due to lunar-solar tides in the Earth's crust and changes in atmospheric pressure. The trend line is shown as a dotted line.

It can be seen that the value of the largest pH anomaly since 2018 has been 0.3 pH units with a duration of approximately 1,500 days (Figure 3), which coincides with the empirical data (12) and (13) with an accuracy of about 20%. Some additional discrepancy may be due to the influence of the preparation processes of other less powerful earthquakes, but closer in location to the preparation zones of foci – such smaller pH anomalies will be discussed later in this article. If we consider that the epicentral distance of the seismogeochemical sites of Tajikistan from the earthquakes of 6.02.2023 was about 3,000 km and the propagation time of the pH anomaly was about 1,500 days, then we can find that the velocity is about 2 km/day. Such velocity values are characteristic of deformation waves propagating during seismotectonic earthquake preparation processes [Bykov 2005 ; Gorbunova and Sherman, 2012; Karimov, 2020; Katok,1991; Mirzoev and Azizova, 1982]. Therefore, it can be assumed that groundwater plays the role of a stress carrier in the propagation of deformation waves as the most dynamic, mobile component of the Earth's crust and upper mantle. In turn, it can be concluded that empirical dependencies (3), (4), (8), (9) to a first approximation satisfactorily reflect the observed anomalies in pH variations and can be used to analyze pH anomalies for other seismotectonic cycles. For the manifestation of groundwater pH anomalies for seismotectonic earthquake cycles from $7.0 \leq M \leq 7.5$, according to dependence (3), the average radius of the preparation zone should be within 1020-1680 km, the average radius of the focus should be 16-28 km (4). For earthquakes from $6.5 \leq M \leq 7.0$ within 620-1020 km, the average radius of the focus is 10-16 km (4). For earthquakes with $5.0 \leq M \leq 6.5$ in the range of 140-620 km, the average radius of the foci is 2-10 km (4). Let us consider the manifestation of pH anomalies from the zones of formation of the strongest earthquakes in the selected area with $M \geq 6.0$ from December 2019 to 2024, the catalog of which is presented in the table. 4. Based on the known dependences of the size of the foci on the magnitude [Sadovsky, 1987; Dobrovolsky, 1991; Riznichenko, 1976; Dobrovolsky, 1989], earthquake preparation zones [Dobrovolsky,1991; Sadovsky,1984] and manifestations of hydrogeochemical anomalies [Dobrovolsky, 1989] for the period from 2020 to 2024, a circle with a radius of 500 km around the center with geographical coordinates $\varphi^0 = 38^0$ (E),$\lambda^0 = 68^0$ (N) was selected for the observation area, located between all observation sites (Figure 1). The parameters of earthquake foci were determined based on earthquake catalogues [Rikitake, 1983]; Catalogues of Russian academy of sciences, The Geofon catalog, URL;Catalog of the American Geophysical Survey]. According to empirical data, the average radius of the zone of inhomogeneity of crustal strains is 380 km or more, and the average size of the foci is more than 12 km (Table 2). The choice of earthquakes with the highest magnitudes is advisable to consider primarily because the areas and, consequently, the linear dimensions of the zones of their preparation are several times or orders of magnitude greater than for earthquakes with lower magnitudes, and, therefore, pH anomalies should be most pronounced. The dates (year-date-minute) of the earthquakes, UT (hours-minutes-seconds), *h* – the depths of the hypocenters, Ms – the magnitude of the surface waves, and mb – the magnitude by volume waves are drawn in Table 4. Data on earthquakes from 6.0 ≥ M ≥ 4.8, the epicenters of which were within a radius of 200 km from seismogeochemical stations for 2020-2024, are presented in the Table 5. To compare the earthquake characteristics, shown in the Table. 4, with the manifestations of pH anomalies, let us consider the time series obtained from the data of seismo-geochemical sites in the observation area (Figures 3-6). The drawings are arranged according to the time scale.

Table 4: Catalog of earthquakes with a magnitude ≥ 6.0 with epicenters within a radius of 500 km from the sites.

№	Date, Time	φ, ^{0N}	λ, ^{0E}	h, км	mb (Ms)	Region	Sites' epicentral distance, km			
							Yavroz	Obigarm	Khodja-Obigarm	Shaam-bary
1	2019-12-20 11:39:50	36.49	70.59	200	6.6	Hind., Afg.	260	240	370	290
2	2020-06-16 01:30:47	37.89	72.31	120	6.1	Taj. (Taj.)	320	270	365	370
3	2021-07-10 02:14:45	38.95	70.68	33	6.2 (5.9)	Afg., Taj.	150	100	190	210
4	2022-05-12 10:27:42	38.14	67.04	10	6.2 (5.2)	S-W Uzb.	220	270	190	165
5	2023-02-23 00:37:40	38.18	73.20	20	6.7 (7.1)	Taj. (Sarez)	400	355	445	470
6	2023-03-22 20:07:45	39.55	69.90	10	6.1 (5.6)	Taj. (Matcha)	115	85	130	160
7	2023-05-03 09:51:20	36.52	70.73	190	6.0	Hind., Afg.	265	240	310	300
8	2023-08-05 16:01:49	36.50	70.81	200	6.0	Hind., Afg.	270	250	310	300

Table 5: Catalog of earthquakes with 6.0 ≥M ≥ 4.8 with epicenters within a radius of 200 km from the stations.

№	Date, Time	φ, ^{0N}	λ, ^{0E}	h, км	mb (Ms)	Region	Sites' epicentral distance, km			
							Yavroz	Obigarm	Khodja-Obigarm	Shaam-bary
1	2020-08-13 18:07:16	38.61	69.88	10	5.0	Taj.	70	-	-	-
2	2021-12-01 03:46:11	38.82	70.04	10	4.9	Taj.	85	25	-	-
3	2022-04-19 22:44:41	39.08	70.53	10	5.3	Taj.	-	90	-	-
4	2023-01-20 03:46:05	39.03	70.54	10	4.9	Taj.	-	85	-	-
5	2024-03-31 03:46:05	39	71	10	5.0	Taj.	-	80	-	-

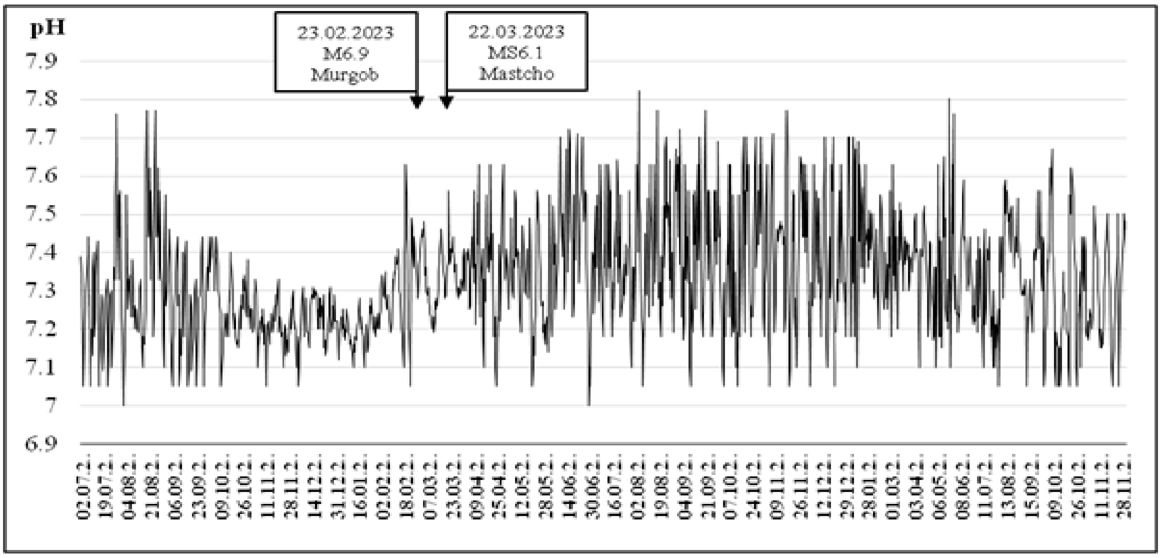

Figure 4: pH parameter run in the site Yavroz site from January 2021 to 2024 (dd. mm. yy)

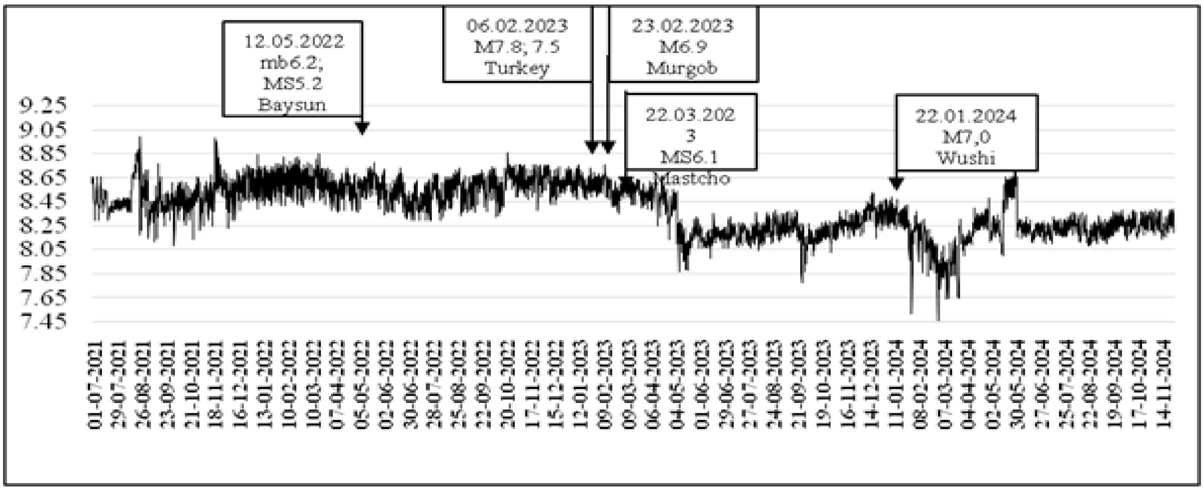

Figure 5: pH parameter run in the site Khoja-Obigarm from February 2020 to 2024 (dd. mm. yy).

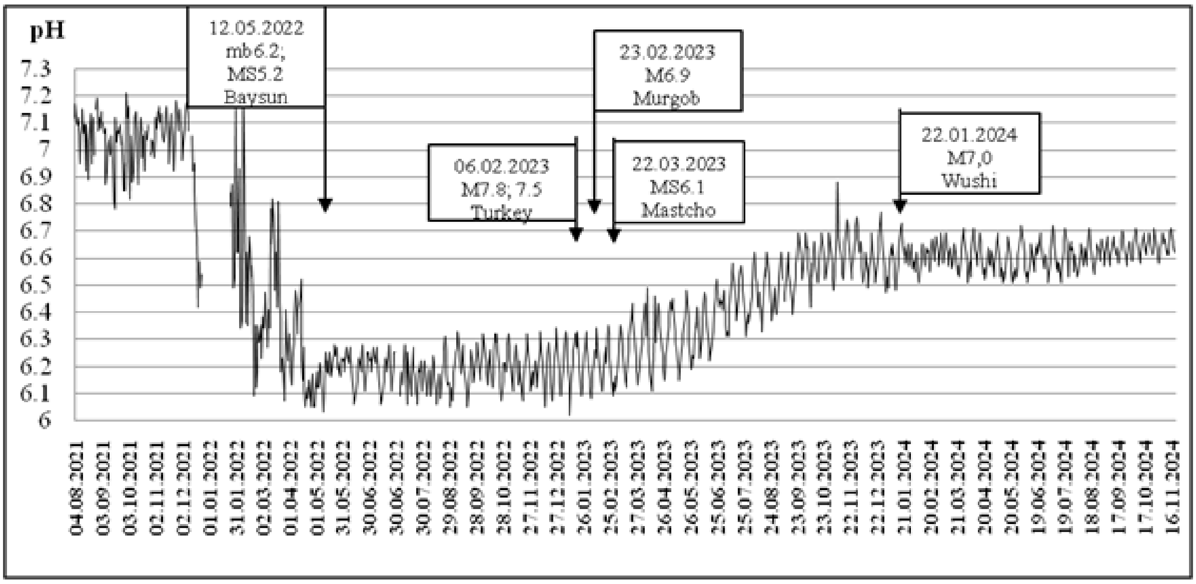

Figure 6: pH parameters run in the site Shaambary from January 2019 to 2024 (dd. mm. yy).

It can be noted that for all these earthquakes with M ≥ 5.0, the epicentral distances to the stations exceeded the average diameter of their foci D0, however, all entered the zones of formation of inhomogeneities of the Earth's crust D, and therefore it can be expected that the corresponding pH anomalies will have the longest durations of more than 215 days (Table 2). To solve inverse geophysical problems and establish a correspondence between local anomalies in pH variations and specific seismotectonic processes of earthquake formation and decay, let us consider tables of summary earthquake data selected based on solving direct geophysical problems (Table 2-5, Figures 3-6). First of all, let us pay attention to the possibility of the preparation of earthquakes with the largest magnitudes in anomalous pH variations during the observation period under consideration with foci in the Upper mantle numbered 1 on 20.12.2019 with M =6.6 and the Sarez crustal, 6, on 23.2.2023 with M= 6.7 (7.1)

For the Upper Mantle earthquake of 20.12.2019 the duration of the anomalies should be at least 1.5 years and therefore it was not possible to analyze pH anomalies completely. Only on the Obigarm site data one can observe the pH value decrease by 0.5 units since March 2019. The pH bay-shaped pH anomaly lasting about 550 days from July 2021 to February 2023 anomaly on the Obigarm time run graph corresponds to the preparation terms of the Matcha earthquake 22.03.2023 with M 5.8 (Figure 3). According to Table 3, such an anomaly coincides in duration with mid-term anomalies in the debit well flow rate. Apparently, a bay-shaped anomaly from August 2022 to March 2023 with a duration of about 300 days was superimposed on this anomaly, which could be attributed to the mid-term stage of preparation for the local Matcha earthquake of 22.03.2023. Indeed, according to table 5, the duration of the orbit should have been about 300 days. The same pH anomaly in the period from August 2022 to March 2023, lasting about 300 days, was noted according to Yavroz site data and it can also be attributed to the preparation of the Matcha earthquake on 22.03.2023. The same two bay-shaped anomalies, from September 2021 to April 2023 and from July 2022 to March 2023, but with a positive sign, appeared according to Khoja-Obigarm site data (Figure 5), can be considered the preceding earthquakes of 23.2.2023 and 22.3.2023.

The anomalies at Shaambary station began earlier than at other stations, in February 2022 (Figure 6). After the anomaly began, the Baysun earthquake on 12.05.2022 occurred with M

6.2 (5.2), with a relatively shallow foci at a depth of about 10 km, and a crustal earthquake with far distant epicenter in the South-Eastern Afghanistan. The epicenter of the first was located closest to Shaambary station, at a distance of 165 km (Table 4), the epicenter of the second is at very large distances from the stations at 550-600 km. Therefore, it is worth considering an earlier occurrence of the anomaly found on Shaambary site as the result of the preparation of the Baysun earthquake. According to the empirical data in Table 4, the duration of the anomaly should have been about 230 days, but in reality, it was about 180 days, which can be explained by the relative remoteness of the epicenter and, as a result some delay in the deformation waves.   According to the Obigarm site in January-February of 2019 there was a decrease in pH by 1.0 and several bay-like anomalies appeared from December to March 2021 and two anomalies with durations of 1 and 2 months from February to July 2021. The last anomaly with duration of about 220 days can be associated with the long-term stage of preparation for the crustal earthquake on 7.10.2021 with M 6.2 in the border region of Tajikistan and Afghanistan, which is in satisfactory agreement with the duration of 230 days in Table 4. As for other shorter anomalies, they can be attributed to the influence of earthquake preparation on 20.12 .2019 and 16.6. 2022, with relatively distant hypocenters.   During the observation period under review, other anomalies in pH variations were found, but they are small compared to those described. This is consistent with the well-known empirical dependences of anomaly characteristics on magnitude, epicentral and hypocentral distances to observation sites: the larger the earthquake and the closer the forming center to the observation stations, the stronger the pH anomalies that appear at longer distances and the more their duration. Following the least square method, the empirical dependence of long-term pH anomalies on the magnitude for the seismically active territory of Tajikistan in the first approximation has been obtained (Figure 7):

$$T\,[days] = \; 0.46M \,-\, 0.51.$$

Date	M	T, days
21.08.2019	5.2	150
21.09.2019	4.5	30
24.01.2020	5.5	50
20.04.2020	4.2	10 (?)
29.01.2020	5.6	150
10.07.2021	6.2	165
5.10.2021	5.4	120
12.05.2022	6.2	190
22.03.2023	6.1	210
23.02.2023	7.1	650

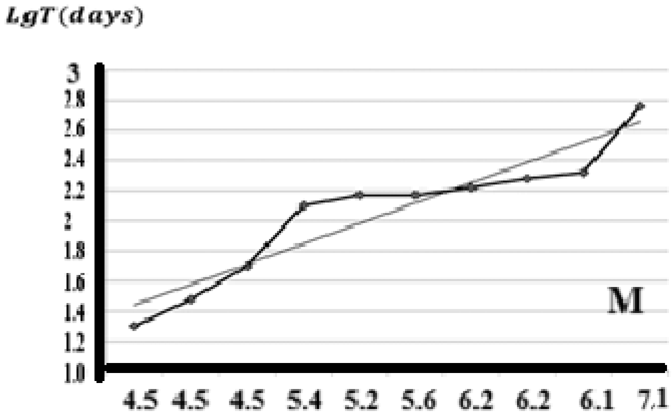

Figure 7: Empirical dependence of the duration of the long-term pH anomaly on the magnitude of Earthquake

6. Conclusions

During observations from 2019/20 until 2024 the anomalies were obtained in variations of the pH parameter of underground thermo-mineral waters in four sites Tajikistan, Obigarm, Khoja-Obigarm, Shaambary and Yavroz, which, according to well-known empirical spatial and temporal dependencies, can be interpreted as long-, mid- and short-term signs of the preparation of tectonic earthquakes. The observation results confirm the nature of the dependence of the duration of pH anomalies on the magnitude of the forming earthquake foci and the hypocentral distance: the larger the earthquake is preparing, the more anomalies in pH variations appear at greater distances. The closer the emerging focus is to the observation stations, the longer their duration. At the stage of earthquake preparation, the acidity of the water decreases, and increases slightly by the time of the main shock. The empirical dependence of the long-term duration of the pH anomaly variations on the magnitude of the upcoming earthquake as the first approximation has been derived for the Tajikistan seismically active areas. The anomalies of pH variations in the preparation of local crustal earthquakes are most regularly manifested while the Upper Mantle Hindu Kush earthquakes are the least regular.

References

Abramov V.Yu., Dolginov E.A. (2013).New data on the influence of lunar phases on earthquakes // *Bulletin of the RUDN University, Engineering Research series*, 2013, No. 2, pp. 37-43 (in Russ.).

Anderson D.L., Whitcomb J.H. (1973). Dilatation model of earthquake forecasting // Conference proceedings. On the tectonic problems of the San Andreas fault system. *Stanf. Univ. Publ.,* vol. 13, pp. 417-426.

Babaev A.M., Mirzoev K.M. (1976), Seismogenic zones of Tajikistan. In: Seismotectonics of the South of the USSR. Ed. by I.E. Gubin. M.: *Science Publ*., pp. 105-117. (in Russ.)

Baratov R.B., Bosler G.I., Becker Ya.A. and others (1981). The Earth's crust and mantle of Tajikistan. Dushanbe: *Donish Publ*., 284 pp. (in Russ.).

Borovkov, Yu. A. *Geomechanics: textbook. Saint Petersburg*: Lan Publ., 2020. 356 p. (in Russ.).

Burtman V.S.(2013), Geodynamics of Pamir-Punjabi syntax , *Geotectonics*, No. 1, pp. 36-58. (in Russ.).

Bykov V.G.(2005) Deformation waves of the Earth: concept, observations and model. *Geology and Geophysics*, vol. 46, No. 11, pp. 1176-1190 (in Russ.).

Dietrich J.H. (1977), Time-dependent friction and sliding mechanics *Materials of the 2nd conference. Experimental studies of rock friction applied to earthquake forecasting. Menlo Park, California*, pp. 389-445.

Dobrovolsky I.P. (1991), *Theory of tectonic earthquake preparation, Moscow: Nauka Publ., 1991, 219 pp. (in Russ.).*

Dobrovolsky I.P.(1989), Deformation of the Earth's crust during earthquake preparation *.Earthquake forecast. Dushanbe, Moscow*: Donish Publ., issue 11, pp. 25-37. (in Russ.).

Dobrovolsky I.P., and Zubkov S.I. (1989), On the processing and presentation of data on earthquake precursors *Earthquake forecast. Dushanbe, Moscow*: Donish Publ., issue 11, pp. 38-51. (in Russ.).

Fusailov I.A. and R.A. Musin (1982), Editors. *The lithosphere of the Pamirs and Tien Shan*.248 pp.: Fan Publ., (in Russ.).

Gorbunova E.A., and Sherman S.I. (2012) Slow deformation waves: fixation, parameters, geodynamic Analysis (Central Asia) . *Pacific Geology*, vol. 31, No. 1,pp. 18-25.

Gubin I.E.(1960), Patterns of seismic manifestations on the territory of Tajikistan. *Moscow: Institute of Physics of the USSR Academy of Sciences,* 463 pp. (in Russ.).

Gubin I.E. and Zakharov S.A.(1983), Editors.Tectonics of the Tien Shan and Pamir, Moscow, 200 pp: Nauka Publ. (in Russ.).

Ishchuk A., Bendik R., Rybin A., Molnar P., Khan M. A., Kuzikov S., Mohajer S., Saidullaev U., Iliyasiva Z., Shchelochkov G., Zubovich A.V. (2013), Kinematics of the Pamir and Hindu Kush regions according to GPS geodesy data . J. Geophys. Res., Solid Earth, p. 118.

Karimov F.H. (2020),Seismogeophysical analysis of the December 7, 2015 Sarez earthquake with M7.2 in Tajikistan. Proceedings of the Institute of Geology, Earthquake Engineering and Seismology of the Academy of Sciences of the Republic of Tajikistan, vol.3. *Proceedings of the scientific and practical conference, dedicated to the 70th anniversary of the Khait earthquake on July 10, 1949 in Tajikistan*, 2020, 101-123. (in Russ.).

Karimov F.H., Salomov N.G., Starkov V.I., Starkova E.Ya., ShozieevSh.P. (2017), Seismogeophysical studies on the territory of Tajikistan and problems of earthquake forecasting, *Geo Risk*, No. 1, pp. 20-28. (in Russ.).

Katok A.P. (1991), On the interrelation of crustal and upper mantle earthquakes in the South of Central Asia , *Physics of the Earth*, No. 12, pp. 3-11. (in Russ.).

Kissin I.G. (2009),Fluids in the Earth's crust. *Moscow: Nauka Publ*., 328 pp. (in Russ.).

Kuksenko V.S. (1984), Kinetic aspects of the destruction process and the physical foundations of its forecasting ,*Earthquake forecast. Dushanbe*, Moscow: Donish, vol. 4, pp. 8-20. (in Russ.).

Kulagin V.K., Halimova H.Z. (1982), Migration of medium-magnitude earthquake foci in the epicentral zones of the Vakhsh region of the Tajik SSR and identification of their occurrence sites, *Earthquake forecast*. Chief editor M.A. Sadovsky. Dushanbe: Donish, No. 1, pp. 56-73. (in Russ.).

Latynina L.A., Vasiliev I.M. (2001), Deformations of the Earth's crust under the influence of atmospheric pressure , *Physics of the Earth*, No. 5, pp. 45-54 (in Russ.).

Lukk A.A., Junga S.L. (1988), *Geodynamics and stress-strain state of the lithosphere of Central Asia. Dushanbe: Donish Publ*., 234 pp. (in Russ.).

Medvedev S.V., Sponkhoyer V.V., Karnik V.V. (1965), The scale of seismic activity – MSC-64. *Moscow: MGK Academy of Sciences of the USSR.* (in Russ.).

Metivier L., De Viron O., Konrad P.S., Renaud S., Diament V., Patau G. (2009), Evidence of earthquakes caused by tides of solid earth *, Earth and Plan. Sc. Let.*, 278, pp. 370-375.

Mirzoev K.M. (1982), The main features of Tajikistan's seismicity, *Earthquake forecast.* Ed by M.A. Sadovsky. Dushanbe: Donish Publ., No. 1, pp. 14-37. (in Russ.).

Mirzoev K.M., Azizova A.A. (1982), Statistical patterns of grouping crustal earthquakes in Tajikistan , *Collection: Earthquakes of Central Asia and Kazakhstan. Dushanbe*: Donish, pp. 48-68. (in Russ.).

Myachkin V.I., Kostrov B.V., Sobolev G.A., Shamina O.G.(1975), Fundamentals of source physics and earthquakes precursors, *In: Physics of the earthquake source*. Moscow: Nauka Publ., pp. 6-29. (in Russ.).

Nur A. (1972) Dilatancy, pore fluids and warning about changes in the passage time of t_S/t_P , *Bulletin of the Seismological Society of America*, vol. 62, pp. 1217-1222.

Pshennikov K.V. (1965), The mechanism of occurrence of aftershocks and inelastic properties of the Earth's crust, *Moscow: Nauka Publ*., 88 pp. (in Russ.).

RiznichenkoYu.V.(1976), Crustal earthquake source size and seismic moment. In: Research on Earthquake Source Physics, *Moscow: Nauka*, pp. 9-27. (in Russ.).

Sadovsky M.A., AvsyukYu.N., Barsukov O.M., Belousov V.V., (1984), and others , Fundamentals of earthquake forecasting. Ed. by M.A. Sadovsky. *Dushanbe-Moscow: Donish Publ*., № 3, 216 pp. (in Russ.).

Sadovsky M.A., Bolkhovitinov L.G., Pisarenko V.F. (1987), Deformation of the geophysical environment and the seismic process. *Moscow (Moscow): Nauka Publ*., , 101 pp. (in Russ.).

Scheidegger A.E. (1981), Physical aspects of natural disasters. *M: Nedra Publ*., 232 pp. (translation from English, in Russ.).

Smirnov V.B., Ponomarev A.V. (2020), Physics of transient seismic regimes. *Moscow: RAS*, 412 pp. (in Russ.).

Todt F.(1967), Corrosion and corrosion protection. *Leningrad: Khimiya Publ*., 709 pp. (transl. from English, in Russ.).

Nikonov A.A.(1977) Holocene and modern movements of the Earth's crust. *Moscow: Nauka Publ*., 240 p. (in Russ.).

Salomov N.G., Mirzoev K.M., Popova G.D.(1982) Search for geochemical precursors of earthquakes at the Dushanbe geophysical site. *Earthquake Forecast*, No. 1, pp. 219-241. (in Russ.).

Muskhelishvili N.I., Some basic laws of the mathematical theory of elasticity. *Moscow:NaukaPubl*.,1966.708p. (in Russ.).

Panasyuk V.V.(1968) The ultimate equilibrium of brittle bodies with cracks. *Kiev: Naukova Dumka*, 246 p. (in Russ.).

Rikitake T.(1983), Earthquake Forecasting and Warning. Tokyo: *Center for Academic Publications of Japan*; Dordrecht, Boston, *Lancaster: Reidel,* 402 pp., ISBN 90 277 1218 2.
.

References are made of the following Catalogs:

Catalog of the Geophysical Survey of the Russian Academy of Sciences, Obninsk, URL: www.gsras.ru

The Geofon catalog, URL: www.geofon.gfz-potsdam.deCatalog of the American Geophysical Survey, http://earthquake.usgs.gov

About the authors

Karimov Farshed Hilol, Doctor of Phys.-Math. Sciences, Chief of the Lab., Institute of Geology, Earthquake Engineering and Seismology, National Academy of Sciences of Tajikistan (NAST), Dushanbe, Tajikistan. E-mail: farshed_karimov@rambler.ru

OlimovShodruzAmirqul, Engineer oftheseismical and geophysical monitoring's network of the Institute of Geology, Earthquake Engineering and Seismology, NAST, Dushanbe, Tajikistan. E-mail: seismtadj@rambler.ru

Olimov Bahrom Qosim, Head of theseismical and geophysical monitoring's network of the Institute of Geology, Earthquake Engineering and Seismology, NAST, Dushanbe, Tajikistan. E-mail: seismtadj@rambler.ru

About the first author and the keynote speaker

e-mail: fhkarim85@gmail.com

Prof. Farshed H. Karimov is the Chief of the Laboratory of Geology and Seismology Tajikistan. He has done extensive work on Earthquake related studies. Took part at the implementation of a highly sensitive magneto metric network for earthquake researches in the Tajikistan seismic region, carried out geomagnetic variations data processing and interpretation (Institute of Earthquake Engineering and Seismology), Exploration-Methodical Geophysical Expedition, Academy of Sciences of the Republic of Tajikistan.

He acted as an expert member of many disaster reduction projects in Tajikistan besides involved in taking part in activities related to seismic hazard and risk and Law on Protection of earthquakes.

His activities spread to promote the development of academic and scientific relations of Tajikistan with the foreign universities and also as Scientific manager of a number of Projects like UNDP, DIPECHO-V in "Strengthened capacity of schools, hospitals and clinics in Dushanbe capital.

Prof Farshed is also an active researcher on Glaciers. His work involves Glacier Dynamics modeling. In 2021 Professor had organized an expedition to Pamirs' glaciers and it turned out very successful. Space images helped to see pictures of glaciers.

In the ionospheric field, he is in interaction with Prof. Obid Alimov, who conducts the ionospheric observations. He has published 400 scientific and engineering papers, theses, reports discourses.

ISSN: 2395-0064

Special Issue IJEAR Vol. 11 No 2 : **February 2025**

Proceedings of International Conference on Electronics and Advances in Science & Technology, (IConEAST-24)

Nov. 8-9, 2024

Towards mitigating natural hazards for a better humanosphere

Venue : Gauhati University, India

Continuous long-term analysis on earthquake-related Total Electron Content (TEC) signals across the Mediterranean region

Roberto Colonna[1,2], Carolina Filizzola[3,2], Nicola Genzano[4],Karan Nayak[5], and Valerio Tramutoli[1,2]

[1]School of Engineering, University of Basilicata, Potenza, Italy;
[2]Space Technologies and Applications Centre (STAC), 85100 Potenza, Italy;
[3]Institute of Methodologies for Environmental Analysis, National Research Council, Tito Scalo (PZ), Italy;
[4]Department ABC (Architecture, Built Environment and Construction Engineering), Polytechnic of Milan, 20133 Milan, Italy;
[5]Faculty of Earth and Space Sciences, Autonomous University of Sinaloa, Mexico.

Article History : *1st received: 24.12.2024   Final : 29.1.2025*

Abstract:

This study examines the correlation between Total Electron Content (TEC) anomalies and seismic activity in the Mediterranean area over a continuous 19-year period (2002–2021). Key methodological inputs were classified and optimized through simulations, resulting in an improved interquartile range (IQR) method for anomaly detection. The optimized method was applied to identify TEC anomalies correlated with seismic events, with rigorous statistical validation highlighting the robustness of the approach. Results indicate that seismic events of magnitude >5.5 can influence the ionosphere up to 90 days prior to the event and within a 1250 km radius.

Keywords: *Ionospheric anomalies, Total Electron Content (TEC), Seismic activity, Optimized IQR method, Magnitude-space-time (MST) domain.*

1. Introduction

Seismic prediction remains one of the greatest challenges in geophysics [Yu and Ma, 2021], with significant societal and economic implications [Huang et al., 2021]. Precursor phenomena, such as ionospheric anomalies, offer a promising avenue for earthquake

ISSN: 2395-0064

prediction [Luo, 2024]. During the last decades, the field has evolved from isolated case studies to comprehensive multi-year analyses, driven by technological advancements in satellite data [Marchetti et al., 2022] and machine learning techniques [Pwavodi et al., 2024]. Among theionospheric anomalies, variations in the Total Electron Content (TEC) have emerged as one of the most investigated parameters due to their sensitivity to geophysical disturbances, including seismic activity [Uyanık et al., 2023; Nayak et al., 2024; Devi et al., 2020].

The ionosphere, influenced by complex interactions between terrestrial, geomagnetic, andsolar processes [Pulinets et al., 2022; Colonna and Tramutoli, 2021], presents a noisy environment where identifying potential seismic-related signals requires robust methodologies and comprehensive datasets[Colonna et al., 2023]. In this context, Global Ionospheric Maps (GIM), derived from Global Navigation Satellite System (GNSS) constellations, provide global TEC measurements with sufficient spatial and temporal resolution for detecting large-scale ionospheric disturbances.

This study builds on the Interquartile Range (IQR) method, a statistical approach widely used to identify TEC anomalies (e.g. [Chen et al., 2024; Rasheed et al., 2024]). By integrating 19 years of TEC with seismic event records and solar/geomagnetic activity indices, the research focuses on refining anomaly detection methods and validating them over long-term datasets. This work specifically focuses on identifying large-scale seismo-ionospheric effects in the Mediterranean region and following the methodological approach proposed by [Colonna et al., 2023], addresses the challenges of handling ionospheric noise, optimally set the magnitude-space-time (MST) domain of correlation between anomalies and seismic activity, optimizing detection thresholds, and validating results across seismic and non-seismic periods.

2. Observations

2.1. Data Sources

TEC data were extracted from GIMs provided by the Center for Orbit Determination in Europe (CODE). These maps cover the Earth's surface in grid cells of 2.5° latitude by 5° longitude. For this study, 8 GIM pixels spanning the Italian region (latitude 37.5N°–47.5N°, longitude 7.5E°–17.5E°) were analyzed (Figure 1).

Seismic event data were sourced from the European-Mediterranean Seismological Centre (EMSC) catalog. The analysis focused on earthquakes of magnitude ≥5 occurring within a spatial radius of 2200 km from the GIM grid cells, encompassing events from 2002 to 2021.

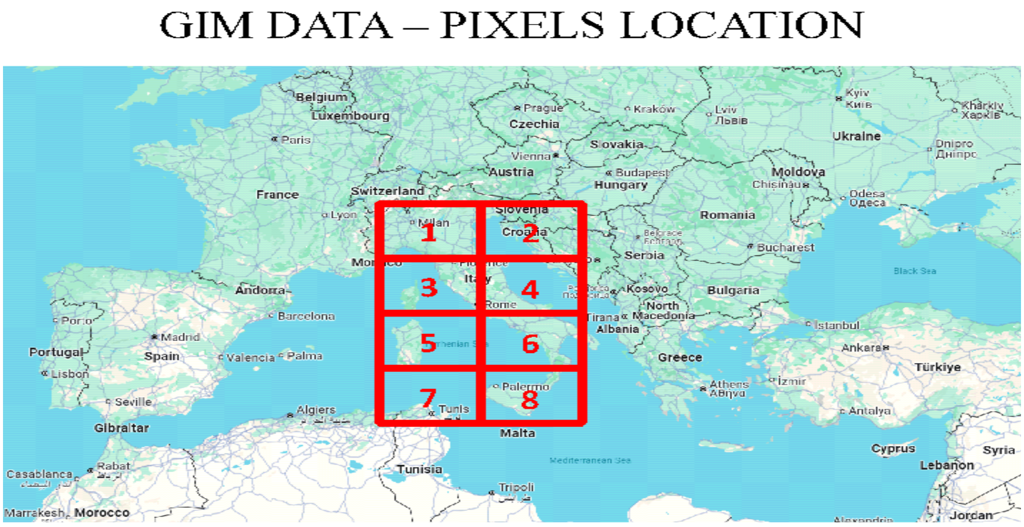

Figure 1: GIM data – Pixels location in the Italian region used for Total Electron Content (TEC) analysis.

Solar activity was quantified using the F10.7 solar flux index, while geomagnetic disturbances were measured via the Dst index. These indices were used to filter out noise unrelated to seismic activity.

In the IQR method, distinct threshold values were applied for positive and negative anomalies. The method was implemented using the following equivalent formulation, which enhances its efficiency for long-term applications (eq. 1).

$$IQR_{INDEX} = \left|\frac{\Delta TEC}{IQD}\right| \quad \text{with: } Kp \geq IQR_{INDEX} > Kn \qquad (1)$$

where:

− ΔTEC = TEC – MM is the deviation of the TEC from the moving median (MM);

− IQD (Interquartile Deviation) is defined as: MM–LQ if ΔTEC<0 and UQ–MM if ΔTEC>0;

− MM, UQ and LQ are, respectively, the moving median, the upper quartile, and the lower quartile calculated from TEC values measured over the same time interval and geographical location during the previous *n* days;

− *Kp* and *Kn* are thresholds for positive and negative anomalies, respectively.

The study progressed through three phases.

2.1.1 Phase1: Selection and Classification

Key methodological IQR and MST domain inputs were selected, set and classified based on their effectiveness in distinguishing seismic-related TEC anomalies.

IQR inputs included:

- Threshold values: distinct values for positive and negative TEC deviations.
- Width of the IQR moving window: 15 days vs. 27 days.
- Persistence criterion: any criterion vs.criterion of anomaly persistence for more than 8 hours.
- Filter for geomagnetic activity: any filter vs. |dst| < 20 nT.
- Filter for solar activity: any filter vs. F10.7 < 200 s.f.u. and IQR-based variable threshold.

The variable threshold filter for solar activity utilizes the F10.7 index, applying the IQR method to ensure that sudden changes in TEC caused by abrupt variations in solar activity are correctly identified as such, rather than being misinterpreted as potential seismic anomalies (see eq. 2).

$$F10.7_{INDEX} = \left| \frac{F10.7 - MM_{F10.7}}{IQR_{F10.7}} \right| < K_{F10.7} \qquad (2)$$

– $MM_{F10.7}$is the 27-day Moving Median associated to each F10.7 under investigation (in the same time-slot).

– $IQR_{F10.7}$is the 27-day interquartile range associated to each F10.7 under investigation (in the same time-slot).

– $K_{F10.7}$is a variable threshold given by the average of the thresholds Kp and |Kn| assigned to the IQR_{TEC} index.

MST domain inputs included:

- Magnitude: M5+ vs. M5.5+ vs. M6+.
- Radius from epicenter: R <Dobrovolsky radius vs. R < 1000 km vs. R < 1250 km; R < 2200 km.
- Depth filter: any filter vs. hypocenter depth greater than 50 km (exclusion criterion).
- Anomaly Time Window (ATW):±15 days vs.±30 days vs−90 days.
- The ATW is the period starting from the occurrence of an earthquake during which any detected anomaly is classified as a true positive (TP).

The classification process utilized the positive likelihood ratio (LR+):

$$LR+ \quad = \frac{TPR}{FPR} \qquad (3)$$

Where TPR and FPR are respectively the True and False Positive Rate, i.e. the number of true or false positives detected by the method weighted for the time in which they can occur. LR+ acts as a metric indicating the strength of correlation between anomalies and seismic events. With over 1.5 million simulations, the input parameters were classified based on their performance (see Table I).

Table I: Positive likelihood ratio (LR+) simulations showing the performance of tested inputs for detecting TEC anomalies correlated with seismic events.

TESTED INPUT CATEGORIES		N° OF SIMULATIONS ON THE TIME SERIES
IQR INDEX INPUTS (20-YEAR TIME SERIES)		16
MST DOMAIN INPUTS (20-YEAR EQ CATALOGUES)		72
N° OF PIXELS		8
Kp VALUES (UPPER THRESHOLDS)	From 1 to 33 in steps of 2	17
Kn VALUES (LOWER THRESHOLDS)	From -1 to -19 in steps of 2	10
TOTAL N° OF 20-YEAR TIME SERIES MATCHED		**1.566.720**

2.1.2 Phase 2: Optimization and Application

Inputs identified as most effective during Phase 1 were used to refine and generate the final detection method. This Optimized IQR Method was applied continuously over the full 19-year dataset, without temporal interruptions, encompassing both periods of seismic activity and periods of seismic inactivity.

2.1.3 Phase 3: Statistical Validation

The detected anomalies statistical significance was evaluated using the binomial distribution law:

ISSN: 2395-0064

$$RP(X \geq TP) = \sum_{TP}^{TA} (TA\ TP)\, p^{TP} (1 - p)^{FP} \tag{4}$$

Where TA, TP and FP are respectively the Total Anomalies, True Positives and False Positives detected and p is the probability of randomness of a single TP, which is given from the ratio between the Cumulative ATW (CATW) and the whole time (WT), investigated. This approach estimated the probability of random correlation between TEC anomalies and seismic events.

3. Results

Classification

The success rates (performance) measured using the LR+ index for the tested inputs of each investigated methodological variable are shown in Figure 2.

In addition, the optimal positive (Kp) and negative (Kn) thresholds for anomaly detection were determined through LR+-based simulations. The resulting values were Kp = 15 and Kn = -11.

4. Application

The most effective inputs were subsequently used to develop the final Optimized IQR method for anomaly detection, which was applied using GIM-TEC data from a single pixel over Italy (Pixel 4 of Figure 1).Figure 3 illustrates the trend of the IQR index, seismic activity, and the corresponding anomalies detected throughout the 19-year study period.

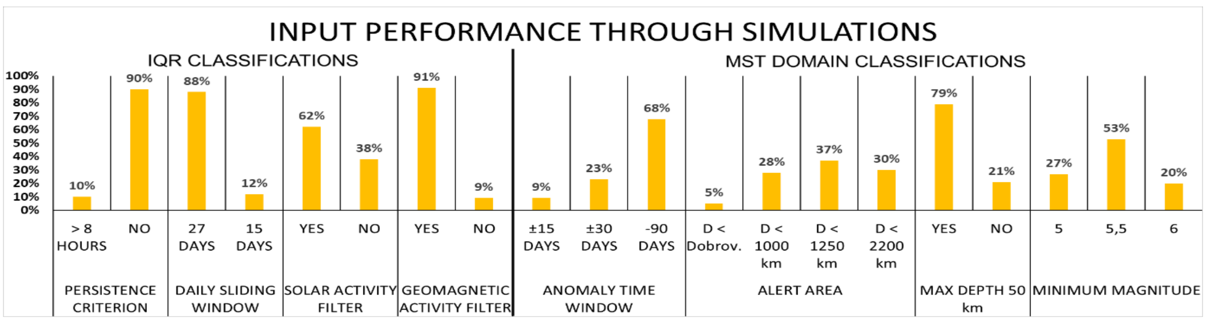

Figure 2: Performance metrics for tested methodological inputs in anomaly detection using the LR+ index.

ISSN: 2395-0064

Special Issue IJEAR Vol. 11 No 2 : **February 2025**

Proceedings of International Conference on Electronics and Advances in Science & Technology, (IConEAST-24)

Nov. 8-9, 2024

Towards mitigating natural hazards for a better humanosphere

Venue : Gauhati University, India

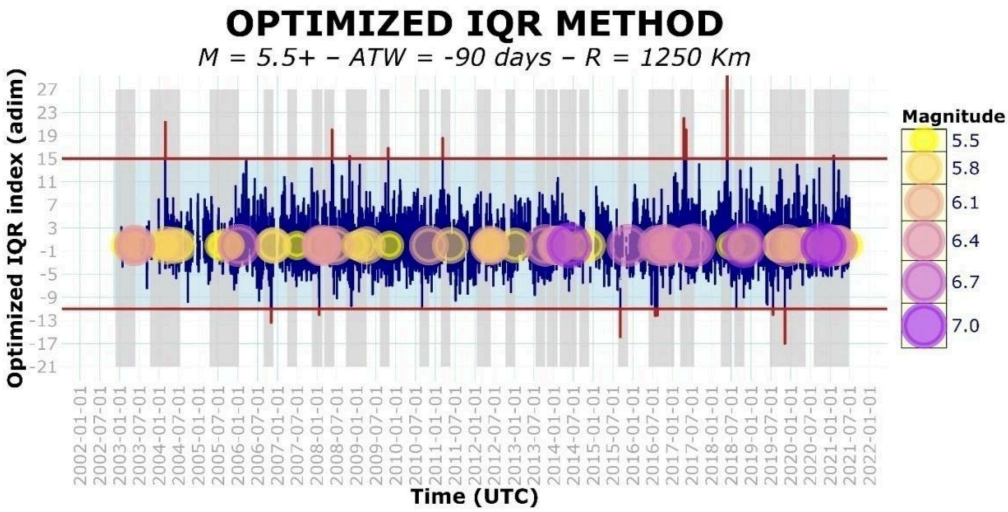

Figure 3: Temporal evolution of the optimized IQR index throughout the 19-year analysis period, along with the seismic activity occurring in the area.Blue line: Optimized IQR index; Red vertical lines: Identified Anomalies; Horizontal lines: Thresholds; Colored circles: Earthquakes with M5.5+, depths < 50 km, and within 1250 km from the monitored point;Gray vertical bands: Anomaly Time Windows (ATWs), defined as the 90 days preceding each seismic event.

The optimized IQR method identified 22 TEC anomalies across the Mediterranean region, all of which were true positives as they occurred within the Anomaly Time Windows (ATWs) – represented by the vertical gray bands in Figure 3 – up to 90 days before earthquakes of magnitude > 5.5, with zero false positives. The total number of seismic events within the MST domain was 70. Of these, 38 were non-alerted events, while 32 were associated with at least one anomaly. Including duplicates (i.e., seismic events linked to more than one anomaly), the 22 anomalies alerted 41 earthquakes. The presence of alerts for the 38 non-alerted events in certain instances couldn't be verified due to data unavailability caused by the application of solar and geomagnetic filters.

Figure 4 (a) and Figure 4 (b) show, respectively, the spatial distribution of the 32 alerted seismic events based on their distance from the TEC measurement point (center of Pixel 4) and the temporal distribution of the identified anomalies relative to the time distance from the

41 associated seismic events. The three radii in Figure 4 (a) were estimated to make the three areas equivalent to each other.

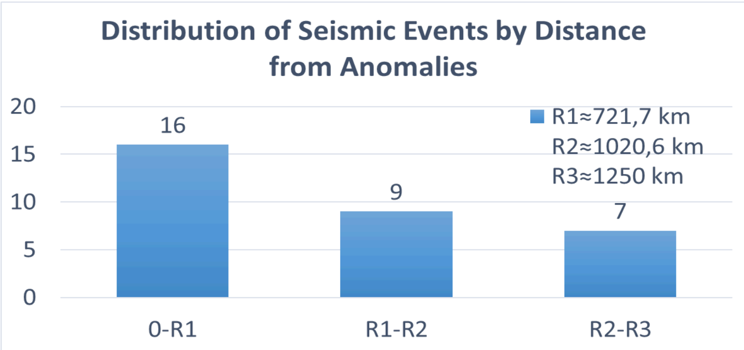

(a)

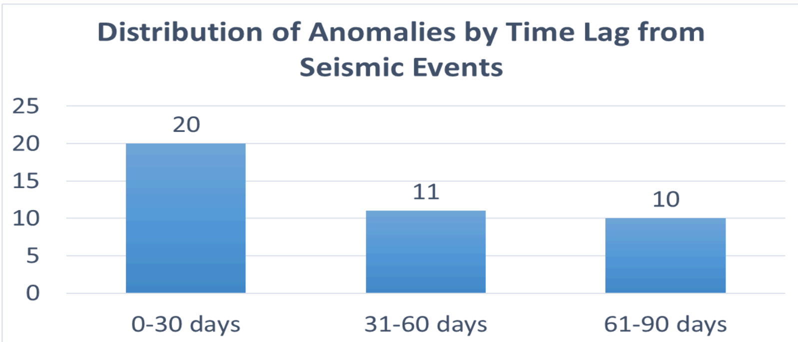

(b)

Figure 4: (a) Spatial distribution of alerted seismic events relative to the TEC measurement point (Pixel 4); (b) Temporal distribution of TEC anomalies with respect to associated seismic events.

The exact spatial location and magnitude of the 32 earthquakes falling within the Anomaly Time Windows (ATWs) during the 19-year analysis period are shown in Figure 5.

Special Issue IJEAR Vol. 11 No 2 : **February 2025**

Proceedings of International Conference on Electronics and Advances in Science & Technology, (IConEAST-24)

Nov. 8-9, 2024

Towards mitigating natural hazards for a better humanosphere

Venue : Gauhati University, India

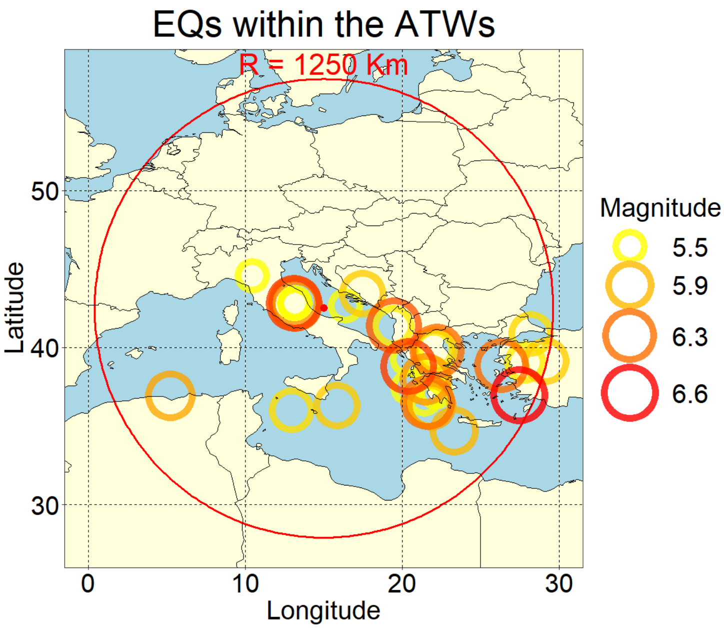

Figure 5: Spatial locations and magnitudes of 32 seismic events falling within Anomaly Time Windows (ATWs) during the 19-year analysis period.

5. Validation

The probability of random correlation between each detected anomaly and the related seismic events (p) was calculated as the ratio ofCATW to WT, yielding a value of 0.512317. Consequently, the probability of random correlation for all 22 detected anomalies with the alerted seismic events (RP) was calculated to be 4 in 10 million, underscoring the robustness of the methodology (see eq.5).

$$RP(X\geq 22) = \sum_{22}^{22}(22\ 22\ )0.512317^{22}(1\ -\ 0.512317)^{0} = 4.07\bullet 10^{-7} \quad (5)$$

***Key Observations about IQR method*:**

- Optimal Thresholds: Distinct thresholds for positive and negative TEC deviations improved true positive anomaly detection.
- Noise Reduction: Solar and geomagnetic filters enhanced signal clarity, isolating seismic-related anomalies.

- Persistence criterion: Short and intense anomalies were found to correlate significantly better with seismic activity compared to persistent phenomena.
- Sliding window: A 27-day sliding window outperformed the 15-day window in detecting seismo-ionospheric effects.

Key Observations about MST domain:

- Spatial Range: seismic-anomalies were detected within 1250 km of the earthquake epicenter.
- Depth Dependency: Earthquakes deeper than 50 km were less likely to produce detectable ionospheric effects.
- Temporal Patterns: TEC anomalies often preceded seismic events by weeks or months.
- Minimum magnitude: M5.5+ earthquakes were more likely to affect the ionosphere.

The analysis of the space-time distribution of the alerted seismic events highlights a significant increase in detection frequency using the optimized IQR method as the spatial and temporal proximity between earthquakes and anomalies decreases.From the methodological point of view this study confirms the effectiveness of a systematic classification of input variables and rigorous statistical long-term validation in TEC-based anomaly detection [Akyol et al., 2020; Colonna et al., 2023].

6. Conclusion

The high correlation between TEC anomalies and seismic events confirms the potential of ionospheric monitoring as a tool for earthquake forecasting. The optimized IQR method, with its

adaptive thresholds and noise filters, provides a robust framework for detecting seismo-ionospheric effects. The method's sensitivity to large-scale ionospheric effects limits

its ability to detect localized anomalies. Future research will focus on integrating multi-parametric data, using both TEC and thermal infrared (TIR) emission measured at the ground [Filizzola et al., 2022], and testing the method across different geographic regions.

Acknowledgement

We sincerely thank the entire executive committee of the IConEAST-24 conference for their exemplary efforts in organizing this prestigious event. In particular, we are profoundly grateful to Professor Minakshi Devi for extending the invitation to the first author, Roberto Colonna, to join the scientific committee and for the honor of serving as an invited speaker.

References

Akyol, A. A., Arikan, O., &Arikan, F. (2020), A machine learning-based detection of earthquake precursors using ionospheric data. *Radio Science*, 55(11), 1–21.https://doi.org/10.1029/2019RS006931.

Colonna, R., &Tramutoli, V. (2021), A new model of solar illumination of Earth's atmosphere during night-time. *Earth*, 2, 191–207. https://doi.org/10.3390/earth2020012.

Colonna, R., Filizzola, C., Genzano, N., Lisi, M., &Tramutoli, V. (2023), Optimal setting of earthquake-related ionospheric TEC (Total Electron Content) anomalies detection methods: Long-term validation over the Italian region. *Geosciences*, 13, 150. https://doi.org/10.3390/geosciences13050150.

Devi, M., Barbara, A., Patgiri, S., Depueva, A., Oyamas, K., Depuev, V., &Ruzhin, Y. (2019), Perturbation features imprinted on ionosphere by successive clusters of strong earthquakes: Role of atmospheric coupling dynamics. *Geomagnetism and Aeronomy*, 59, 955–970. https://doi.org/10.1134/S0016793219080036.

Filizzola, C., Corrado, A., Genzano, N., Lisi, M., Pergola, N., Colonna, R., &Tramutoli, V. (2022), RST analysis of anomalous TIR sequences in relation with earthquakes occurred in Turkey in the period 2004–2015. *Remote Sensing*, 14, 381. https://doi.org/10.3390/rs14020381.

Huang, D., Wang, S., & Liu, Z. (2021), A systematic review of prediction methods for emergency management. *International Journal of Disaster Risk Reduction*, 62, 102412. https://doi.org/10.1016/j.ijdrr.2021.102412.

Luo, Y. (2024), A critical review of geomagnetic and ionospheric anomalies as earthquake precursors. *IntechOpen*. https://doi.org/10.5772/intechopen.1007474.

Marchetti, D., De Santis, A., Campuzano, S. A., Zhu, K., Soldani, M., D'arcangelo, S., Orlando, M., Wang, T., Cianchini, G., Di Mauro, D., et al., (2022), Worldwide statistical correlation of eight years of Swarm satellite data with M5.5+ earthquakes: New hints about the preseismic phenomena from space. *Remote Sensing*, 14, 2649. https://doi.org/10.3390/rs14112649.

Nayak, K., Romero-Andrade, R., Sharma, G., Lopez, C., Trejo-Soto, M., &Vidal-Vega, A.,(2024), Evaluating ionospheric Total Electron Content (TEC) variations as precursors to seismic activity: Insights from the 2024 Noto Peninsula and Nichinan earthquakes of Japan. *Atmosphere*, 15, 1492. https://doi.org/10.3390/atmos15121492.

Pulinets, S., Ouzounov, D., Karelin, A., & Boyarchuk, K., (2022), Earthquake precursors in the atmosphere and ionosphere: New concepts. *Springer Nature*. https://doi.org/10.1007/978-94-024-2172-9.

Pwavodi, J., Ibrahim, A. U., Pwavodi, P. C., Al-Turjman, F., &Mohand-Said, A., (2024), The role of artificial intelligence and IoT in prediction of earthquakes: Review. *Artificial Intelligence in Geosciences*, 5, 100075. https://doi.org/10.1016/j.aiig.2024.100075.

Rasheed, R., Chen, B., Wu, D., & Wu, L., (2024), A comparative study on multi-parameter ionospheric disturbances associated with the 2015 Mw 7.5 and 2023 Mw 6.3 earthquakes in Afghanistan. *Remote Sensing*, 16. https://doi.org/10.3390/rs16111839.

Yu, S., & Ma, J., (2021), Deep learning for geophysics: Current and future trends. *Reviews of Geophysics*, 59. https://doi.org/10.1029/2021RG000742.

About the first author and the invited speaker

*e-mail:*r.robertocolonna@gmail.com

Dr. Roberto Colonna is an Italian researcher with extensive expertise in remote sensing, geophysics and machine learning. He holds a Ph.D. in *Engineering for Innovation and Sustainable Development*, with a strong background in the analysis of satellite data for earthquake-related studies. He has been involved in several international research projects and scientific conferences, contributing to advancements in Earth observation techniques. His research also includes geospatial analysis applications for environmental monitoring (e.g., forest fire detection, water body monitoring and crop yield prediction)."